

**CONVERTER FOR WIRELESS POWER TRANSFER IN ELECTRIC
VEHICLE BATTERY CHARGING SYSTEM**

By

MASHITAH BINTI MOKHTAR

FINAL PROJECT REPORT

Submitted to the Department of Electrical & Electronic Engineering
in Partial Fulfillment of the Requirements
for the Degree
Bachelor of Engineering (Hons)
(Electrical & Electronic Engineering)

Universiti Teknologi PETRONAS
Bandar Seri Iskandar
31750 Tronoh
Perak Darul Ridzuan

© Copyright 2012

by

Mashitah Binti Mokhtar, 2012

CERTIFICATION OF APPROVAL

CONVERTER FOR WIRELESS POWER TRANSFER IN ELECTRIC VEHICLE BATTERY CHARGING SYSTEM

by

Mashitah Binti Mokhtar

A project dissertation submitted to the
Department of Electrical & Electronic Engineering
Universiti Teknologi PETRONAS
in partial fulfilment of the requirement for the
Bachelor of Engineering (Hons)
(Electrical & Electronic Engineering)

Approved:

Assoc. Prof. Dr. Nordin Bin Saad
Project Supervisor

UNIVERSITI TEKNOLOGI PETRONAS
TRONOH, PERAK

May 2012

CERTIFICATION OF ORIGINALITY

This is to certify that I am responsible for the work submitted in this project, that the original work is my own except as specified in the references and acknowledgements, and that the original work contained herein have not been undertaken or done by unspecified sources or persons.

Mashitah Binti Mokhtar

ABSTRACT

Electric vehicle does not require oil consumption and it does not emit gas pollutants as it uses electrical engine to run its system. Electric vehicle provides the solution for the awareness of the limited fossil fuels and environmental issues such as green house gas emission. The technical solution of the electric vehicle charging system is one of the challenges because it does not have standard solutions. In the future, wireless charging system is the best method of electric vehicle charging system compared to the conventional plug-in or conductive charging as it offers more convenient, faster and user friendly of charging system.

This paper addresses the design of the converter for wireless power transfer in electric vehicle battery charging system. A research studies about electric vehicle charging system was made and all related theories and information are gathered in a literature review. With the pre-planned methodology that was made to guide the project flow, a converter design is develop from a resonant converter basic design approach using PSPICE simulation by determining the current and voltages, in several points of the circuit. The project has proved that by using this method, a variable DC output voltage of the converter can be obtained by controlling the value of the switching frequency. With this characteristic, the objective of the project has been achieved. However, a further research on rectifier for very high frequency should be made to improve the power transfer efficiency which is very significant in the circuit design.

ACKNOWLEDGEMENTS

First of all, I would like to thank Universiti Teknologi PETRONAS (UTP) for giving me a chance to complete my Final Year Project (FYP) throughout two semesters in my final year studies. This is really a golden opportunity for me to challenge myself to apply knowledge in engineering theories as well as gain extra experiences to deal with unexpected problems that are not able to learn from the theory. I also want to take this opportunity to gratefully acknowledge the contribution of several people who helped me in completing this project.

My appreciation records to my supervisor, A.P. Dr. Nordin Bin Saad for giving me an opportunity to conduct my Final Year Project under his supervision. I would like to thank my supervisor for his guidance, support, assistance and advisements throughout these two semesters. I have learned a lot and enjoy doing the project with his willingness to teach, patience to explain and consider understanding.

My special thanks to the co-supervisor, A.P. Dr. Mohamad Bin Awan for his guide and help throughout the completion of the project. Besides, I would like to thank Dr. Nor Zaihar Bin Yahaya for his willingness to share the Microsim 8 PSPICE software and also for sharing the knowledge. I also would like to thank to all other lecturers whom involved directly or indirectly in my project work.

Finally, I would like to thank my fellow friends and family members for their continuous support and concern whenever I needed them. Besides, I am very grateful and thank to other people who have directly or indirectly helping me to succeed the project.

TABLE OF CONTENTS

CHAPTER 1	INTRODUCTION	1 - 3
1.1	Background of Study	1
1.2	Problem Statement	2
1.3	Objective and Scope of the Project	3
CHAPTER 2	LITERATURE REVIEW	4 - 6
2.1	Inductive Power Transfer System	4
2.2	Magnetic Linkage	5
2.3	Resonant Circuit	6
CHAPTER 3	METHODOLOGY	7 - 21
3.1	Project Work	7
3.2	Research Methodology	9
3.3	Activities/Gantt Chart and Milestone for FYP 1	10
3.4	Activities/Gantt Chart and Milestone for FYP 2	11
3.5	Converter Design Work	12
3.5.1	Battery Requirement	12
3.5.2	Block Diagram	12
3.5.3	Resonant Frequency	15
3.5.4	Half -Bridge Parallel Resonant Converter	18
3.5.5	Converter Circuit Configuration	19
3.5.6	Rectifier at Very High Frequency Source	20
3.6	Software and Tools Used	21

CHAPTER 4	RESULTS AND DISCUSSION	22 – 53
4.1	Results and Discussion of RC Circuit	22
4.2	Results and Discussion for Half-bridge PRC	38
4.2.1	Current Switching	39
4.2.2	Lossless Switching	41
4.3	Results and Discussion for Converter Circuit	44
4.4	Results and Discussion for Rectifier at Very High Frequency	53
CHAPTER 5	CONCLUSION AND RECOMMENDATION	55 – 56
5.1	Conclusion	55
5.2	Recommendation	56
	REFERENCES	57
	APPENDIX	59

LIST OF TABLES

Table 1: Gantt Chart for FYP 1 -----	10
Table 2: Gantt Chart for FYP 2 -----	11
Table 3: Specifications for-13 series array lithium ion battery -----	12
Table 4: Parameters with different switching frequency for $F_r=55$ kHz -----	23
Table 5: Parameters with different switching frequency for $F_r = 90$ kHz -----	36
Table 6: Switching losses and conduction losses in switch A and Switch B -----	44
Table 7: Summary of variable DC output voltage -----	52
Table 8: Series of lithium ion battery voltage requirement -----	53

LIST OF FIGURES

Figure 1: Main blocks of an inductive power transfer -----	4
Figure 2: Resonant circuit topologies -----	6
Figure 3: Project activities flow -----	7
Figure 4: Block diagram of battery charging system operation -----	12
Figure 5: Illustration of wireless charging[14] -----	13
Figure 6: Illustration of the suggested converter circuit in real application[14] --	13
Figure 7: Expected circuit diagram -----	14
Figure 8: Resonant circuit basic design with $F_r=55\text{kHz}$ -----	15
Figure 9: Resonant circuit basic design with $F_r=90\text{kHz}$ -----	17
Figure 10: Half-bridge PRC circuit configuration -----	18
Figure 11: Converter circuit configuration-----	20
Figure 12: Rectifier for very high frequency source, V6 -----	20
Figure 13: Voltage output vs switching frequency ($F_r=55\text{kHz}$) -----	23
Figure 14: Current output vs switching frequency ($F_r=55\text{kHz}$) -----	24
Figure 15: Inductor current vs switching frequency ($F_r=55\text{kHz}$) -----	24
Figure 16: Voltage and Current Waveform for $F_s = 100\text{kHz}$ -----	26
Figure 17: Voltage and Current Waveform for $F_s = 110\text{kHz}$ -----	26
Figure 18: Voltage and Current Waveform for $F_s = 120\text{kHz}$ -----	27
Figure 19: Voltage and Current Waveform for $F_s = 130\text{kHz}$ -----	27
Figure 20: Voltage and Current Waveform for $F_s = 140\text{kHz}$ -----	28
Figure 21: Voltage and Current Waveform for $F_s = 150\text{kHz}$ -----	28
Figure 22: Voltage and Current Waveform for $F_s = 160\text{kHz}$ -----	29
Figure 23: Voltage and Current Waveform for $F_s = 170\text{kHz}$ -----	29
Figure 24: Voltage and Current Waveform for $F_s = 180\text{kHz}$ -----	30

Figure 25: Voltage and Current Waveform for $F_s = 190\text{kHz}$ -----	30
Figure 26: Voltage and Current Waveform for $F_s = 200\text{kHz}$ -----	31
Figure 27: Voltage and Current Waveform for $F_s = 210\text{kHz}$ -----	31
Figure 28: Voltage and Current Waveform for $F_s = 220\text{kHz}$ -----	32
Figure 29: Voltage and Current Waveform for $F_s = 230\text{kHz}$ -----	32
Figure 30: Voltage and Current Waveform for $F_s = 240\text{kHz}$ -----	33
Figure 31: Voltage and Current Waveform for $F_s = 250\text{kHz}$ -----	33
Figure 32: Voltage and Current Waveform for $F_s = 260\text{kHz}$ -----	34
Figure 33: Voltage and Current Waveform for $F_s = 270\text{kHz}$ -----	34
Figure 34: Voltage and Current Waveform for $F_s = 280\text{kHz}$ -----	35
Figure 35: Voltage output vs switching frequency ($F_r=90\text{kHz}$) -----	36
Figure 36: Current output vs switching frequency ($F_r=90\text{kHz}$) -----	37
Figure 37: Inductor current vs switching frequency ($F_r=90\text{kHz}$) -----	37
Figure 38: Waveforms of $I_D(M1)$, $I(CSQ1)$, $I(CSQ2)$ and $I(CSQ1)-I(CSQ2)$ -----	40
Figure 39: Waveforms of $I(SD1)$ and $I(SD2)$ -----	40
Figure 40: Waveforms of V_A , $V(SQ1)$ and $I_D(M1)$ -----	41
Figure 41: Waveforms of V_B , $V(SQ2)$ and $I_D(M2)$ -----	42
Figure 42: Switching losses at Switch A (V_A) -----	43
Figure 43: Switching losses at Switch B (V_B) -----	43
Figure 44: Converter output waveform for $F_s=100\text{ kHz}$ -----	45
Figure 45: Converter output waveform for $F_s=110\text{ kHz}$ -----	45
Figure 46: Converter output waveform for $F_s=120\text{ kHz}$ -----	46
Figure 47: Converter output waveform for $F_s=130\text{ kHz}$ -----	46
Figure 48: Converter output waveform for $F_s=140\text{ kHz}$ -----	47
Figure 49: Converter output waveform for $F_s=150\text{ kHz}$ -----	47
Figure 50: Converter output waveform for $F_s=160\text{ kHz}$ -----	48

Figure 51: Converter output waveform for $F_s=170$ kHz -----	48
Figure 52: Converter output waveform for $F_s=180$ kHz -----	49
Figure 53: Converter output waveform for $F_s=190$ kHz -----	49
Figure 54: Converter output waveform for $F_s=200$ kHz -----	50
Figure 55: Converter output waveform for $F_s=210$ kHz -----	50
Figure 56: Converter output waveform for $F_s=220$ kHz -----	51
Figure 57: Converter output waveform for $F_s=230$ kHz -----	51
Figure 58: Converter output voltage characteristic for different F_s value -----	52
Figure 59: Waveform output voltage of the rectifier circuit -----	54

LIST OF ABBREVIATIONS

EV	Electric Vehicle
RC	Resonant Circuit
PRC	Parallel Resonant Converter
IPT	Induction Power Transfer
MOSFET	Metal-Oxide Semi Conductor Field-Effect Transistor
IGBT	Insulated-Gate Bipolar Transistor
PSPICE	Personal Computer Simulation Program with Integrated Circuit Emphasis

CHAPTER 1

INTRODUCTION

1.1 Background of Study

The introduction of electric vehicle (EV) in automobiles has been contributing to improve their efficiency and reduce the production of gas emission that contributes to global warming. Conventional vehicle consumes oil reserves to power its internal combustion engine (ICE) while electric vehicle (EV) uses electrical engine as a replacement of the internal combustion engine (ICE). Electric vehicle (EV) is more environmental friendly as it does not require oil consumption and pollutant emissions free. Furthermore, the source of the electricity for electric vehicle can be generated from a wide range of sources including fossil fuels, nuclear power and renewable sources such as solar power, wind power, and tidal power or any combination of those.

Electric vehicles (EVs) will be gradually launched in the market in the coming years and will to contribute to change the daily life of urban regions [1]. One challenge related with electric vehicle (EV) is the technical solution of the charging system. This paper proposes wireless power transfer for electric vehicle battery charging system as wireless charging is more comfortable as it does not require any cable to connect to the vehicle.

1.2 Problem Statement

1.2.1 Problem Identification

Conventional plug-in charging systems are currently being practiced in electric vehicle battery charging system. Cable is required in order to recharge the vehicle battery. However, plug-in charging system is only suitable to be applied for electric vehicle (EV) that is used for short distance driving range. This is because most electric vehicles (EVs) can only go about 100 – 200 miles before recharging. When traveling a long distance, the electric vehicle (EV) needs to be recharged for several times at the respective charging station because the charging activity can only be executed at the plug-in charging station. This is cumbersome and not user friendly.

In the future, electric vehicle is expected to be the main transportation and will be used worldwide. Since electric vehicle has the potential to be the future vehicle in the next generation, it is best if the charging system could be improved to be more faster, comfortable and user friendly. Using wireless power transfer in electric vehicle battery charging system that is proposed in this paper should improve the electric vehicle charging system in a more convenient way.

1.2.2 Significance of Project

Several rectifier and converter circuits will be used in the wireless power transfer for electric vehicle battery charging system. The rectifier and converter circuits will be designed based on all the required parameters at the load (electric vehicle battery).

By modeling a prediction model of the wireless power transfer in electric vehicle battery charger system, this will prove that the system helps to improve the current plug-in charging system. Wireless power transfer for electric vehicle battery charging system requires electronic converter that provides high efficiency. High switching frequency is needed for high power transfer capability. The wireless power transfer charging system will be modeled in PSPICE for analysis.

1.3 Objective and Scope of the Project

1.3.1 *Main Objective*

Aim of this project is to suggest with converter circuit that can be used for wireless power transfer in electric vehicle charging system. The subobjectives of this project are as listed in the following:

- i. To outline the advantages of wireless power transfer in electric vehicle charging system over current plug-in hybrid electric vehicle charging system.
- ii. To analyze battery requirement in electric vehicle.
- iii. To obtain low losses converter circuit for wireless power transfer in electric vehicle battery charging system.
- iv. To design the resonant converter.
- v. To simulate and analyze the modeled system in PSPICE.

1.3.2 *Scope of Project*

The project will starts with a study about wireless power transfer in electric vehicle battery charging system. After that, the project will proceed to data gathering regarding the battery requirement. Next is to design a converter with high efficiency to transfer power to the electric vehicle battery by modeling the circuit using PSPICE software. Further studies and analysis will be carried out to improve the efficiency of the converter as well as to provide the best performance for wireless power transfer in electric vehicle battery charging system.

CHAPTER 2

LITERATURE REVIEW

2.1 Inductive Power Transfer System

Inductive power transfer is the concept of transferring energy without the need of contact such as using wires to connect the load to the source and is based in the magnetic induction [2]-[7]. There are four major blocks in the basic circuit of inductive power transfer system: a power source, a magnetic link, a resonant circuit and a battery charger.

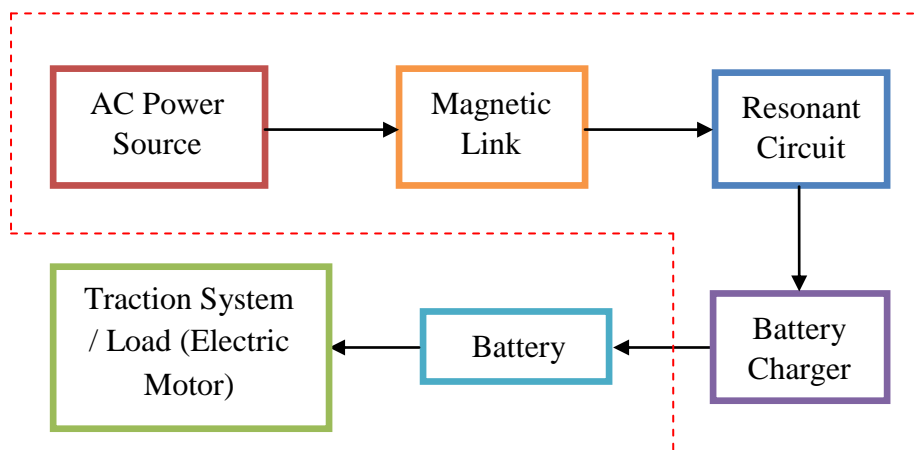


Figure 1: Main blocks of an inductive power transfer

Usually, the circuit is composed with rectifier and inverter. The function of the magnetic linkage is to transfer the power between the power source and the battery charger and is composed of two coils. The resonant circuit is needed to increase the power transfer efficiency because it will compensate the reactive part of total impedance. The battery charger controls the charging process and the changing voltage to the levels accepted by the battery.

2.2 Magnetic Linkage

Magnetic induction is the basic principle behind the magnetic linkage between primary and secondary coils [5], [8]-[12]. When the flux density is equally distributed in a space with same magnetic permeability, it will reach the secondary coil. In Ampere law, wire that composes a coil will produce induce current when an alternating magnetic field is flowing through the coil. This is how the concept of wireless power transmission works. The quality of the linkage between coils is the important factor that needs to be taken into account. Magnetic linkage coefficient, k is use to evaluate the quality. This coefficient relates the linkage flux, which is the flux that connects the two coils, with the dispersion flux, which represents the flux of the primary that does not flow through the secondary coils. This relation can be expressed in the following equation:

$$k = \frac{L_M}{L_p L_s} \quad (1)$$

Where L_M is the mutual induction while L_p and L_s is the self-inductions of primary circuit and secondary circuit.

A traditional inductive power transfer system is indicated by having a magnetic linkage coefficient that varies between 0.3 to 0.6 [13], which is considered a weak magnetic linkage. In order to increase the efficiency of magnetic linkage, two capacitors are used. These capacitors and the magnetic linkage coils establish a tank circuit. Resonant condition can be achieved by tuning the tank circuit since the performance of the charging system is strongly influenced by the tank circuit.

2.3 Resonant Circuit

Two capacitors are introduced to overcome the problem of low magnetic linkage coefficient which cause decreases in the system efficiency. One capacitor is placed in the primary and another one in the secondary to form a resonant circuit with the coils of magnetic linkage. This allows a compensation of the reactive part of the total circuit impedance. In other word, resonance become purely resistive. The condition of resonant is when the energy stored in capacitor equals the energy stored in the inductor. In order to obtain the resonant angular frequency ω_0 , the capacitor impedance will be equal to the inductor impedance as example in the following (assume in the secondary circuit):

$$\omega L_s = \frac{1}{\omega C_s} \Leftrightarrow \omega = \omega_0 = \frac{1}{\sqrt{L_s C_s}} \quad (2)$$

Normally, capacitor is the component used to tune the circuit since the inductor and the frequency are usually fixed parameters. There are four topologies for resonant circuit, which are Series-Series (SS), Series-Parallel (SP), Parallel-Series (PS) and Parallel-Parallel (PP) as shown in Figure 2.

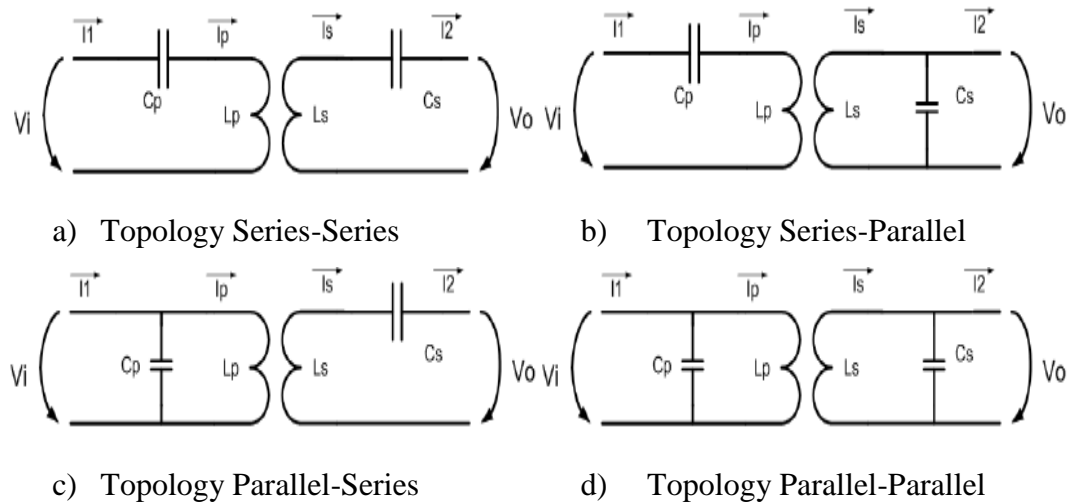


Figure 2: Resonant circuit topologies

CHAPTER 3

METHODOLOGY

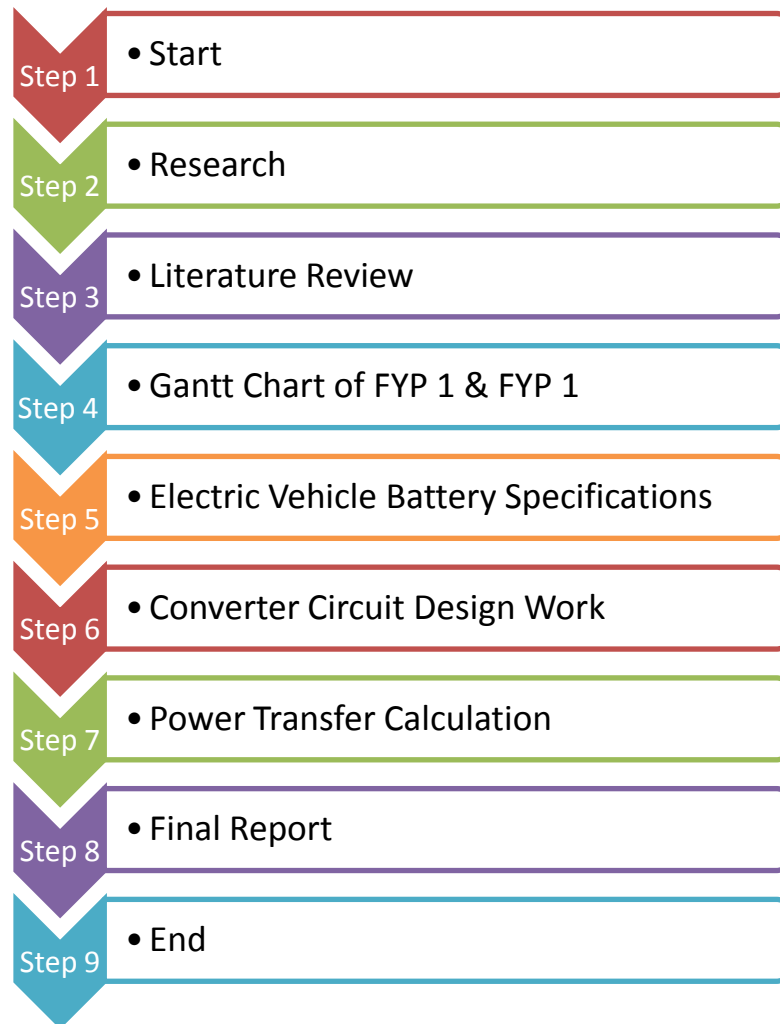


Figure 3: Project activities flow

The project begins with research on several issues related to wireless power transfer in electric vehicle battery charging system. All the information and knowledge then been gathered in the literature review on the electric vehicle studies about the wireless power transfer in the battery charging system which is more convenient and environmental friendly compared to conventional vehicle.

After completed the literature review, the basic studies of wireless power transfer moved onto the classification of electric vehicle battery and its important parameters requirement. Nowadays, there are many types of electric vehicle battery such as lead-acid battery, nickel metal hydride (NiMH) battery and lithium-ion (Li-ion) battery. In this project, 13-series array lithium ion battery is chosen as the reference for battery specification. The battery specification is attached in the Appendix A.

Next, the lossless switching was the typical part in the simulation in the project in order to perform power transfer efficiency calculations. After that, project proceed to the correlation of the mathematical manner which will be fully manipulated in order to design the appropriate converter design of electric vehicle battery charging system. The understanding of power transfer concept is very useful for designing the circuit elements features and the constraint face by the system had give a great engineering challenge.

Finally, all the studies and discussion is compiled and included in this final report. Apart from that, the suggested design of circuit elements features will be further explain and justifies part by part. The operational recommendations also been developed and mentioned in Chapter 5.

3.2 Research Methodology

Research is done in order to gain information regarding the major scope of the project. The sources of the research cover the handbook of electric vehicle and its battery charging system, e-journal, e-thesis and several trusted link.

The steps of research:

1. Gain information of the classification of electric vehicle which focus on power transfer in its battery charging system and comparison of the plug-in charging system with the wireless charging system.
2. List down the challenges of electric vehicle wireless power transfer.
3. Simplify the power transfer concept used.

3.3 Activities/Gantt Chart and Milestone for FYP 1

Details/Week	1	2	3	4	5	6	7	8	9	10	11	12	13	14
Proposing the topic														
Information gathering														
Extended proposal submission														
Analysis														
Develop RC circuit basic design														
Simulation/Modelling														
Proposal Defense														
Draft report submission														
FYP1 interim report submission														

Table 1: Gantt Chart for FYP 1

3.4 Activities/Gantt Chart and Milestone for FYP 2

Details/Week	1	2	3	4	5	6	7	8	9	10	11	12	13	14	15
Analyze the result	■	■	■	■											
Submission of progress report								■							
Design the converter circuit			■	■	■	■	■	■	■	■					
Pre-EDX											■				
Submission of draft report												■			
Submission of dissertation(soft bound)													■		
Submission of technical paper													■		
Oral presentation														■	
Submission of project dissertation (hardbound)															■

Table 2: Gantt Chart FYP 2

3.5 Project Activities

The progress of this project was according to the pre-planned methodology in order to achieve all project sub-objectives. Firstly, the concept and theory of resonant converter been gathered. From the research, the type of the circuit of resonant converter and its calculation of parameters are identified based on the requirements of the electric vehicle battery charger. Then the project proceeds with the modeling and simulation of the parameters using Microsim 8 PSPICE tools.

3.5.1 Battery requirement

The specifications of battery for electric vehicle is obtained and assessed. Lithium ion battery is chosen to be assessed as it is the most commonly used for electric vehicle. The specifications for 13 series array lithium ion battery are shown in Table 3 below. Its specification can be obtained in Appendix A.

Charging mode	107.9 V
Discharging mode – Lower limit	78.0 V
Discharging mode – Nominal limit	97.5 V

Table 3: Specifications for 13-series array lithium ion battery

1 lithium ion battery = 7.5 V

3.5.2 Block Diagram

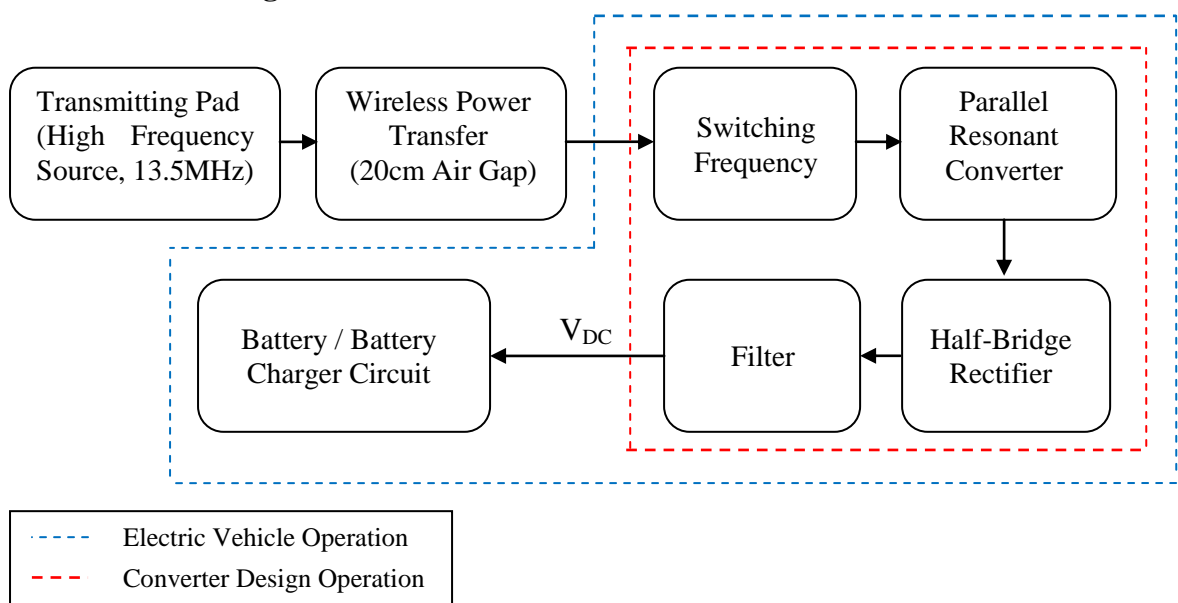


Figure 4: Block diagram of battery charging system operation

Based on the block diagram in Figure 4, the source of the converter will be from a very high frequency (13.5 MHz) AC voltage and the power from the source will be transferred from a primary coil (transmitting pad) to a secondary coil (receiving pad or charging pad). In real application, the transmitting pad will be placed on the ground such as on the garage floor, parking lot or on the road in highways. Meanwhile, the receiving pad will be put under the electric car so that each time the car is parked or used across the road, the battery will be charged automatically. This can be illustrated as in Figure 5 below.

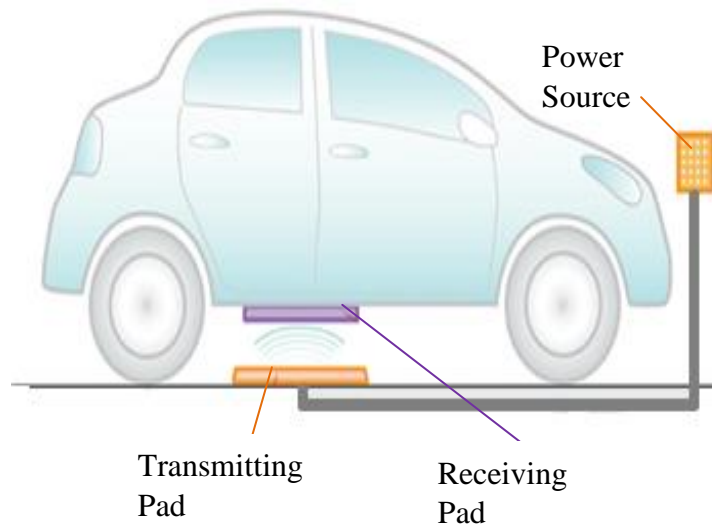


Figure 5: Illustration of wireless charging. [14]

From the receiving pad, a converter circuit will be needed to deliver the power to the battery or battery charging circuit. Therefore, a high switching frequency switch will be needed in order to achieve high power transfer efficiency through the circuit. This project basically is focusing on the design of the converter. This can be illustrated in Figure 6.

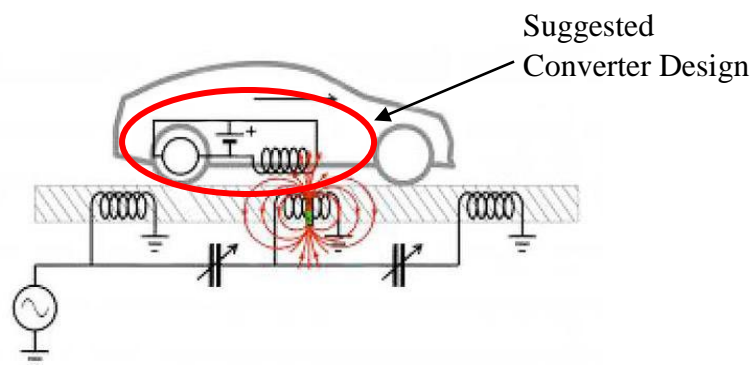


Figure 6: Illustration of the suggested converter circuit in real application. [14]

In order to deal with a high switching frequency which is above resonant (90kHz), the circuit is designed based on basic RC design with a high value of resonant frequency F_r , which is assumed as 90kHz. The calculation of resonant was made and will be shown in Equation (3). Next, after a few analyses is done the parallel resonant converter is designed with half-bridge rectifier to convert the AC voltage into DC voltage. Therefore, a filter is included in order to reduce or eliminate any voltage ripple or noise produce by the circuit which is expected to occur. The lossless switching, current switching, and any other behavior or characteristics that occur is analyzed and included in Chapter 4. The expected full converter design is shown in Figure 7 and it will be compared to the final circuit design that is obtained in Chapter 4.

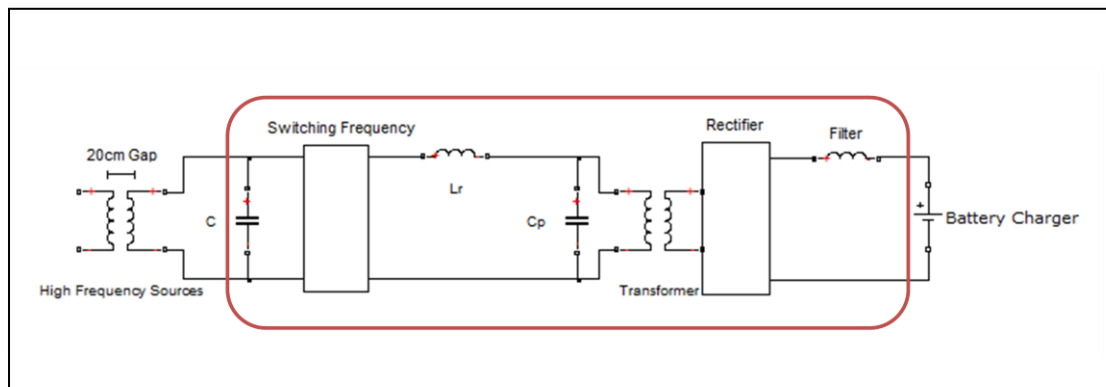


Figure 7: Expected circuit diagram

The expected circuit diagram is expected to produce a variable DC voltage for different switching frequency so that the voltage can be controlled according to its capacity. This is because in real application, voltage discharged of the battery will be varies at the time it is to be charged. It may vary from a minimum voltage requirement, V_{MIN} to maximum voltage requirement, V_{MAX} accordingly. This values are referring to Table 3 and is varies for different number of series of the lithium ion battery. In this project, there are 5 conditions to be checked which are:

- 10-series array lithium ion battery
- 15-series array lithium ion battery
- 20-series array lithium ion battery
- 25-series array lithium ion battery
- 30-series array lithium ion battery

3.5.3 Resonant Frequency

After getting the battery specifications, the design work begun. The design work starts with the resonant circuit basic design. At first, resonant frequency of the resonant circuit design is $F_r = 55$ kHz. The resonant circuit then is analyzed by giving increasing values of switching frequency. The output parameters of the resonant circuit are observed and will be discussed in Chapter 4.

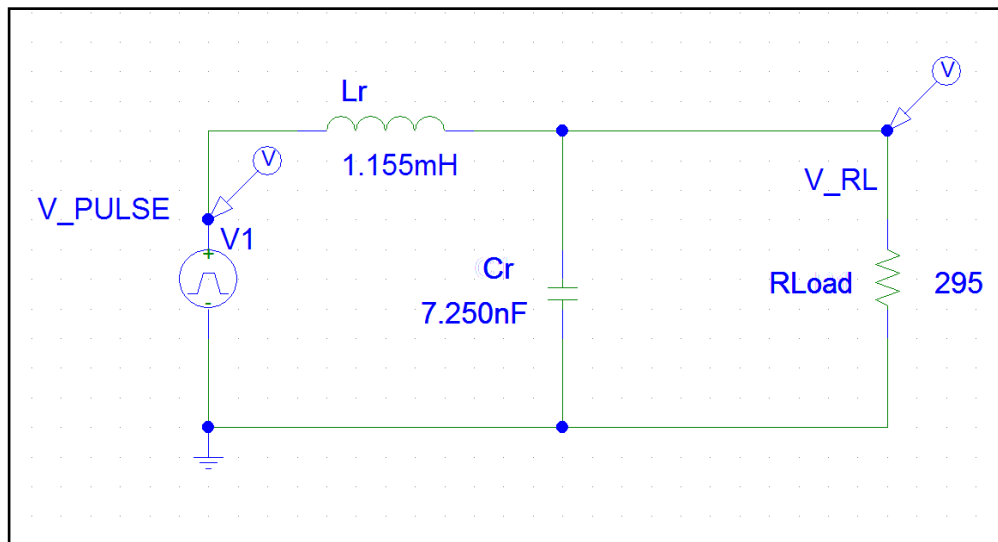


Figure 8: Resonant circuit basic design configuration with $F_r=55$ kHz

The values of L_r and C_r are fixed to get resonant frequency, F_r of 55 kHz. This can be achieved by referring to the formula of resonant frequency.

$$F_r = \frac{1}{2\pi\sqrt{L_r C_r}} \quad (3)$$

- Voltage Pulse Generator Setting for $F_{\text{switching}}$ of 55 kHz :

$$V1 = -170 \text{ V}$$

$$V2 = 170 \text{ V}$$

$$TD = 10 \text{ us}$$

$$TR = 0 \text{ us}$$

$$TF = 0 \text{ us}$$

$$PW = 8.33 \text{ us}$$

$$PER = 16.67 \text{ us}$$

- Inductor

Lower inductor values is needed since the peak to peak current increases linearly with switching frequency chosen for high frequency converter [15].

- Capacitor

Capacitor used to reduce voltage ripple, minimize output noise voltage and to guarantee regulation during transient loads [15].

After a few simulations had been made, a decision was made to change the value of resonant frequency, F_r to 90kHz instead of 55kHz because higher switching frequency, F_s will gives small switching losses which is better to be used. Besides, a high switching frequency will be used in the wireless power transfer battery charging. In fact, 100kHz of switching frequency will be used in the converter circuit because it will give 10us of switching time or period (PER) which it gives more accurate value to be put in the PSPICE software element specification.

This can be obtained using this formula;

$$t_{switching} = \frac{1}{F_{switching}} \quad (4)$$

$$t_{switching} = \frac{1}{100k} = 10us$$

In order to use a new resonant frequency, the suitable value of resonant inductor, L_r and resonant capacitor, C_r need to be determined. The equation of resonant frequency (Equation 3) is used to determine the value of resonant elements. After that, a few analysis need to be done until the circuit gives a square wave of switching frequency with a smooth sine wave output which both give the same value of maximum voltage.

The values of the new resonant elements are;

- 1) Resonant inductor, L_r of 0.7068mH.
- 2) Resonant capacitor, C_r of 4.4244nF.

To check the value of resonant frequency with the new resonant values:

$$F_r = \frac{1}{2\pi\sqrt{L_r C_r}} = \frac{1}{2\pi\sqrt{(0.7068m)(4.4244n)}} = 90 \text{ kHz}$$

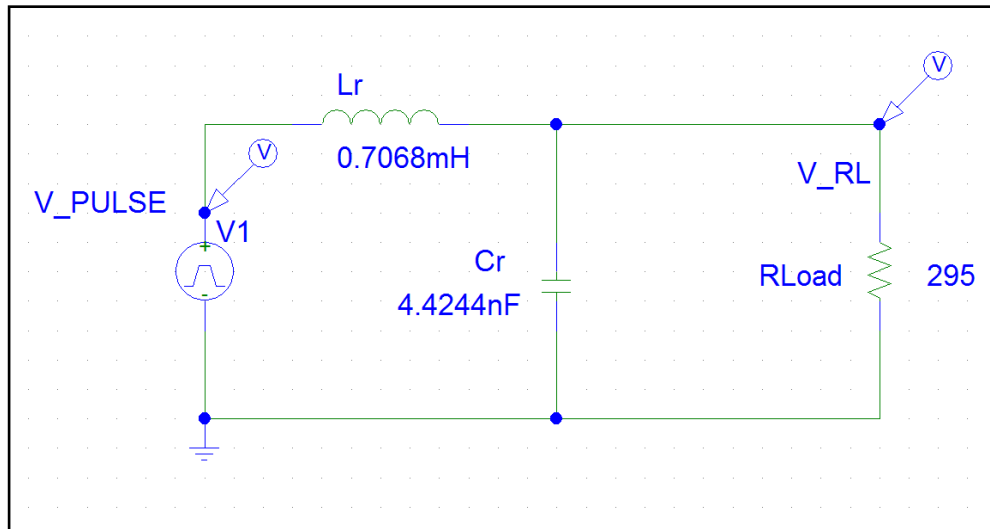


Figure 9: Resonant circuit basic design configuration with $F_r=90\text{kHz}$

- Voltage Pulse Generator Setting for $F_{\text{switching}}$ of 90 kHz :

V1	= -170 V
V2	= 170 V
TD	= 10 us
TR	= 0 us
TF	= 0 us
PW	= 5.5555 us
PER	= 11.1111 us

The output results of the RC circuit with the new resonant values will be shown and further discussed in Chapter 4.

3.5.4 Half-bridge Parallel Resonant Converter (PRC)

After the desired output is obtained from the RC circuit, project is continued by expanding the RC circuit to half-bridge Parallel Resonant Converter. Half-bridge PRC is chose over a full-bridge PRC because half-bridge has no magnetic path gap therefore low stray magnetic field. Besides, frequency received by secondary circuit double basic switching frequency leads to low noise and voltage ripple which are desirable. Therefore, small filter components (L and C) are required.

Other than that, power MOSFET is used to produce two high switching frequencies because it is suitable for a high switching frequency (higher than 100kHz) rather than using Insulated Gate Bipolar Transistor (IGBT) which is only suitable for low switching frequency. In fact, one of the typical applications of power MOSFET is in battery charging.

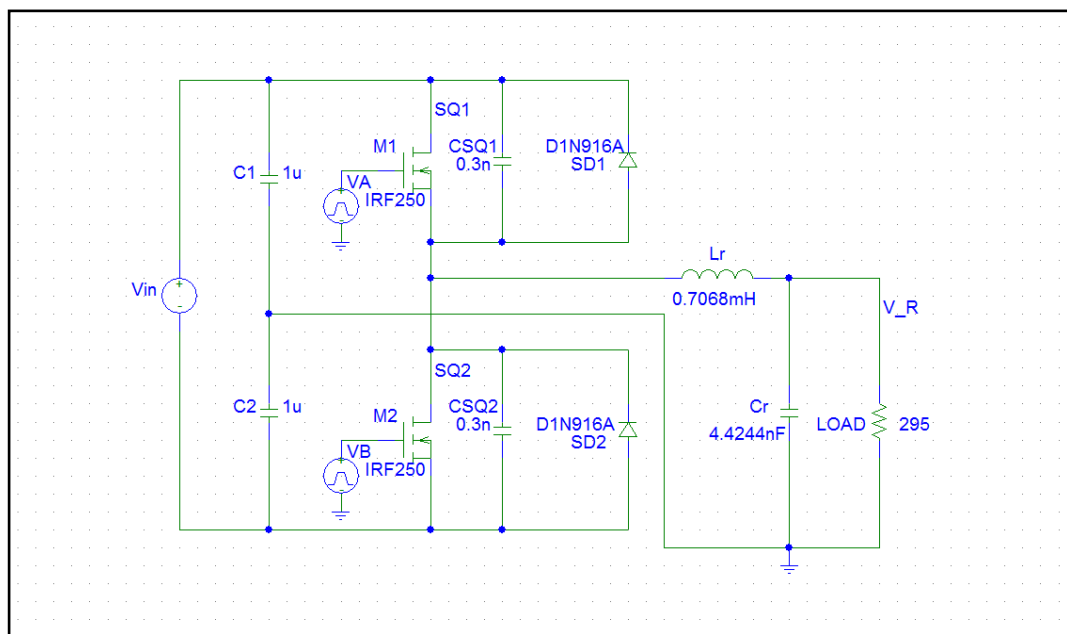


Figure 10: Half-bridge PRC circuit configuration

SWITCHING SPECIFICATIONS

Voltage Pulse Generator Setting for Switch 1 (VA):

V1	= -170 V
V2	= 170 V
TD	= 10 us
TR	= 10 ns
TF	= 10 ns
PW	= 4.98 us
PER	= 10 us

Voltage Pulse Generator Setting for Switch 2 (VB):

V1	= 170 V
V2	= -170 V
TD	= 9.865 us
TR	= 10 ns
TF	= 10 ns
PW	= 5.25 us
PER	= 10 us

3.5.5 Converter Circuit Configuration

After analyzing the half-bridge PRC to get the minimum switching losses, the circuit is expanded by connecting a transformer and rectifier to get a DC output voltage as desired. A small value of filter components is desired in order to obtain low output ripple and noise. This characteristics match with half-bridge PRC that is used in the primary side.

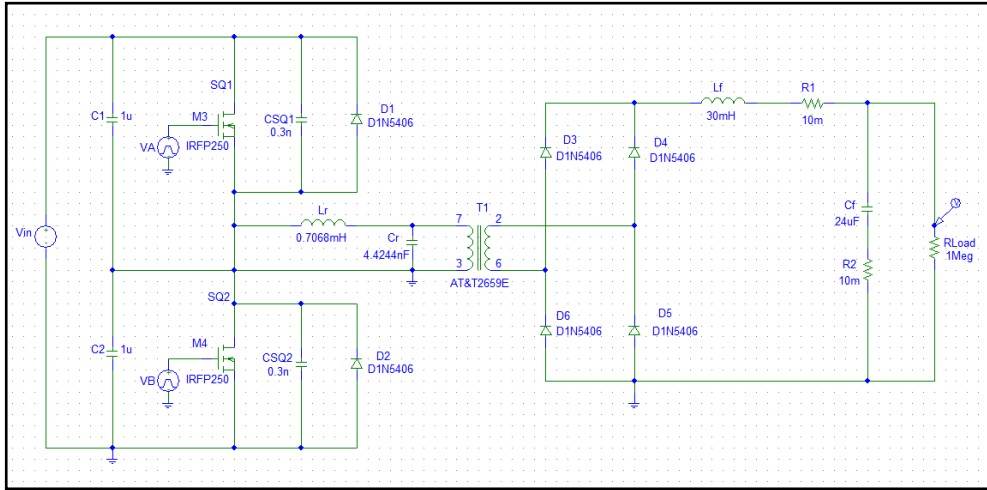


Figure 11: Converter circuit configuration

3.5.6 Rectifier for a very high frequency source

The source of the system would be from a very high frequency which is 13.5MHz so that the power transfer can be done wirelessly at 20cm air gap. In this project, a rectifier circuit is modeled for 13.5MHz frequency source. The desired DC voltage output is according to value of V_{in} used in converter design configuration which is $340V_{AC}$. Below is the circuit diagram of the rectifier.

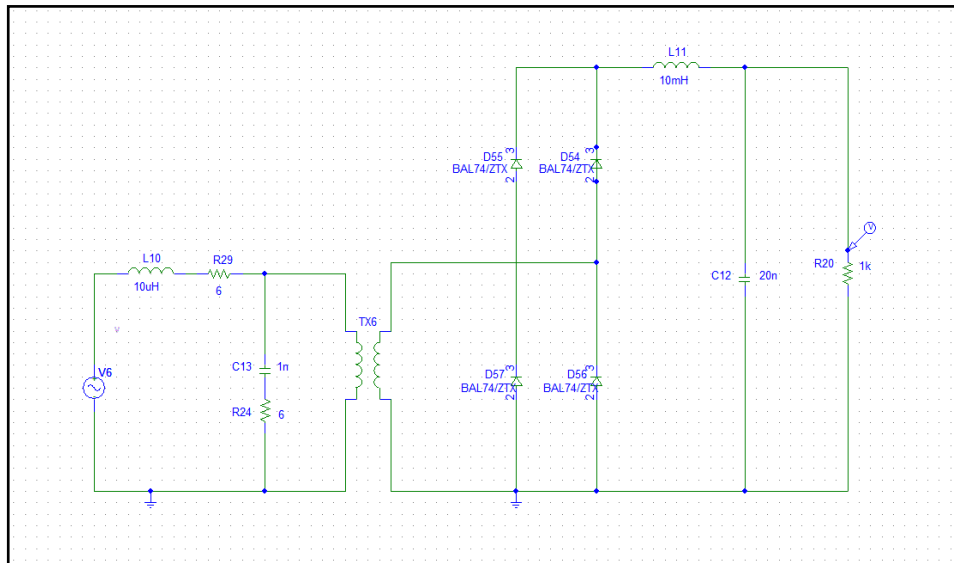


Figure 12: Rectifier for very high frequency source, V6

3.6 Software and Tools Used

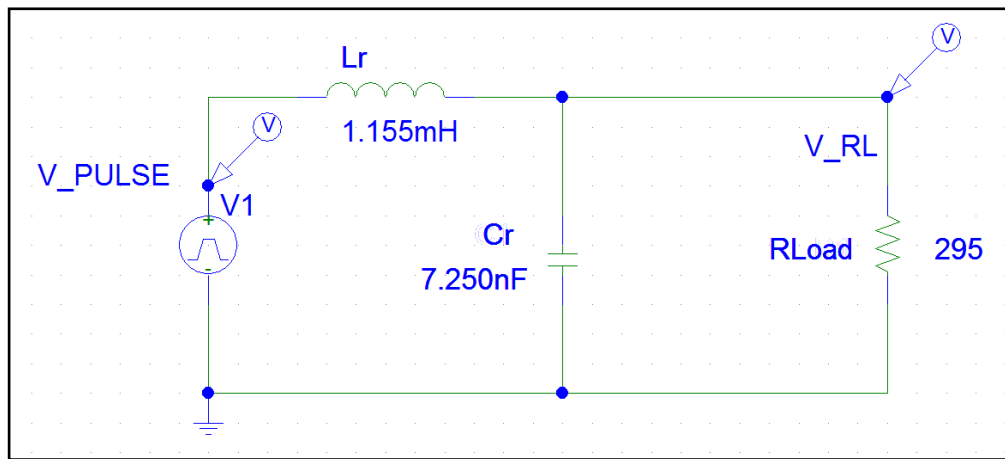
At the beginning of the simulation, the software used is MATLAB Version 2009. After gone through frequent of trial, some elements cannot be able to simulate because of the limitation of MATLAB Toolbox. This student version limits only for certain elements which effect many components are not available. Starting from then, MATLAB Version 2009 does not be used anymore and proceed with Microsim 8 PSPICE software which offers much more components and easy to learn and work on. The project is done by modeling the circuit in Microsim 8 PSPICE software.

CHAPTER 4

RESULTS AND DISCUSSION

4.1 Results and Discussion of RC Circuit

The characteristics of the output voltages and current at the load and current at the inductor are shown for every different switching frequency. The value of resonant frequency is constant which is $F_r = 55\text{kHz}$. Below is the basic RC circuit.



Output characteristics of RC circuit with $F_r=55\text{ kHz}$ is analyzed. The values of the current and voltages at the load also the current at the inductor for RC circuit with $F_r=55\text{ kHz}$ are tabulate in the Table 4.

No.	Frequency (kHz)	V_R (V)	I_R (A)	I_L (A)	
				PEAK	RMS
1.	55	170.0000	0.5762	0.6895	0.4876
2.	65	138.1250	0.4699	0.6462	0.4569
3.	75	110.0000	0.3770	0.5813	0.4110
4.	85	88.1250	0.2995	0.5187	0.3668
5.	95	70.9940	0.2406	0.4637	0.3279
6.	105	58.1250	0.1947	0.4119	0.2913
7.	115	47.1040	0.1601	0.3760	0.2659
8.	125	40.2450	0.1386	0.3313	0.2343
9.	135	34.3750	0.1173	0.3088	0.2184
10.	145	30.1570	0.1012	0.2790	0.1973
11.	155	26.2500	0.0885	0.2625	0.1856
12.	165	22.5000	0.0785	0.2438	0.1724
13.	175	20.6210	0.0712	0.2299	0.1626
14.	185	18.3720	0.0628	0.2117	0.1497
15.	195	16.2370	0.0571	0.2027	0.1433
16.	205	14.5080	0.0516	0.1889	0.1336
17.	215	13.7570	0.0481	0.1750	0.1237
18.	225	12.5000	0.0439	0.1688	0.1194
19.	235	11.7070	0.0375	0.1648	0.1165
20.	245	10.7660	0.0345	0.1575	0.1114

Table 4: Parameters with different switching frequency for $F_r = 55$ kHz

Based on the data tabulated in Table 4, the values of the important parameters at the load and at the inductor are plotted as shown below :

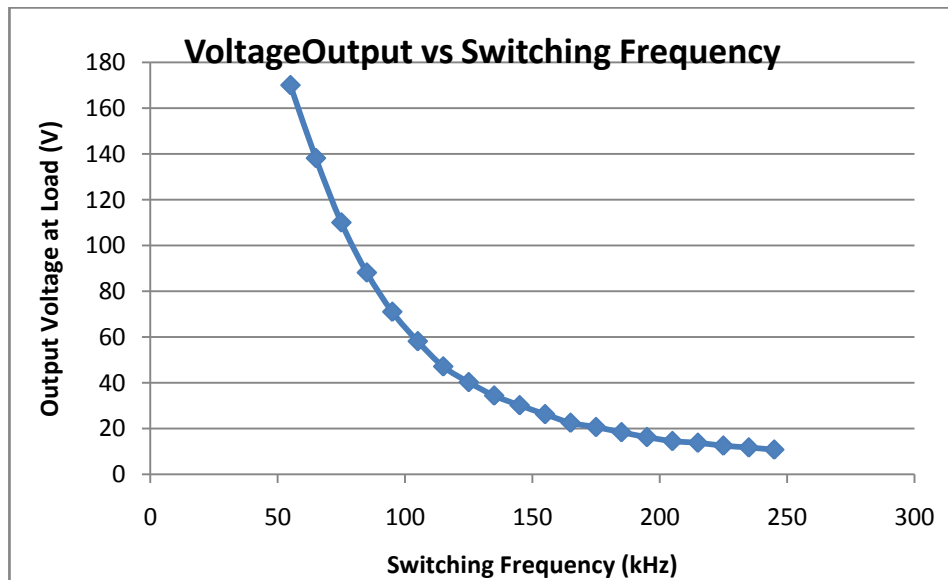


Figure 13: Voltage output vs switching frequency ($F_r=55$ kHz)

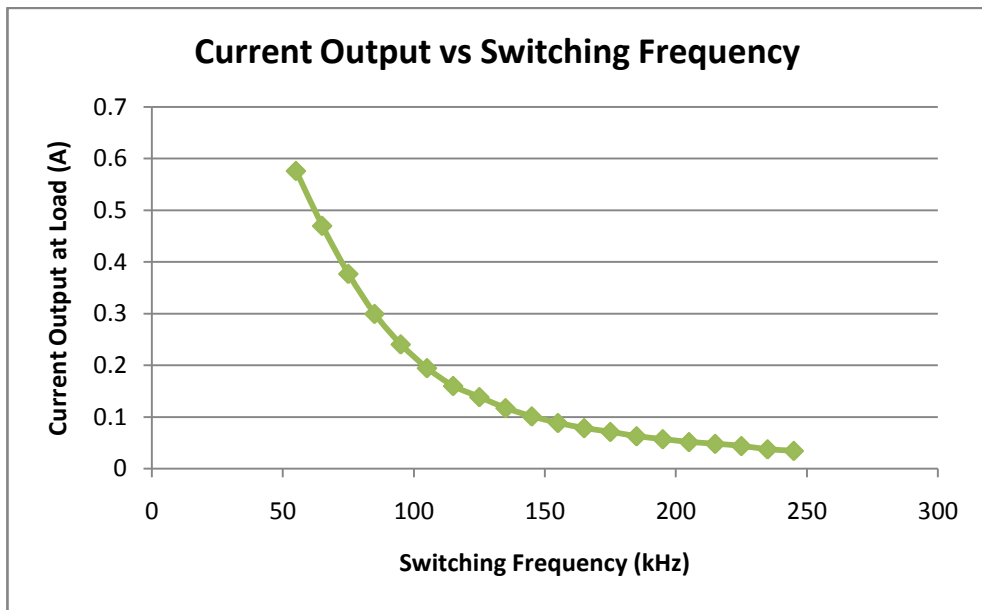


Figure 14: Current output vs switching frequency ($F_r=55\text{kHz}$)

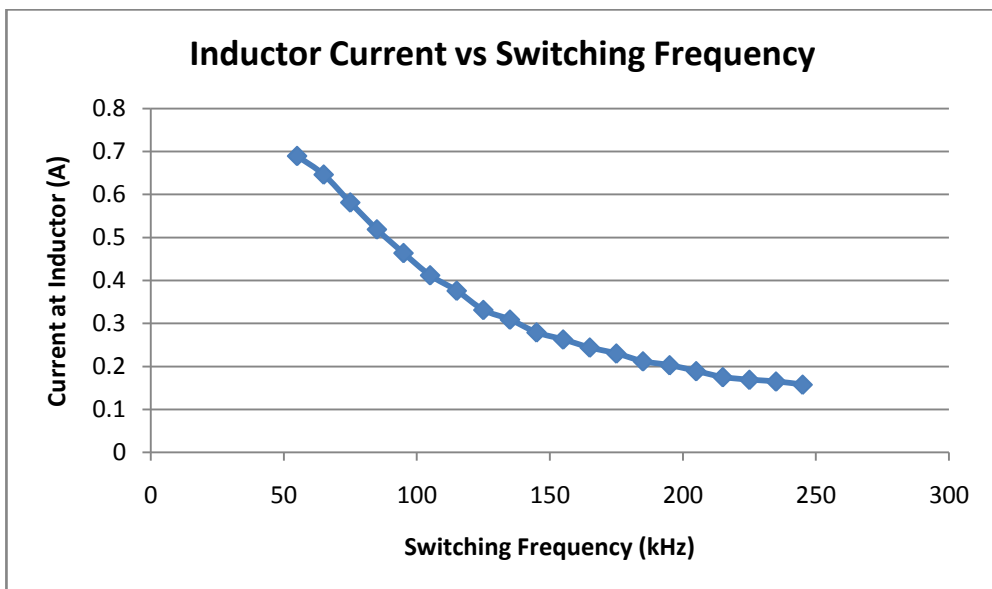
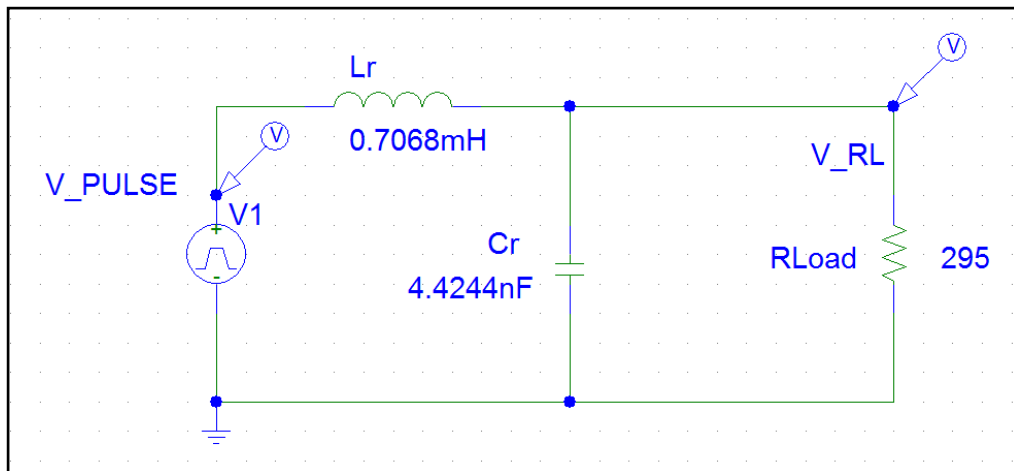


Figure 15: Inductor current vs switching frequency ($F_r=55\text{kHz}$)

Observation is made and the value of the output voltage is varying with different values of switching frequency. Referring to the graph, it proves that the output voltage at the load is decreasing with an increasing value of switching frequency. Notice that when $F_s=225$ kHz, the output voltage reaches 12.5 V. Other than that, values of the current at the load and current at the inductor are also decreasing as the switching frequency is increasing.

As mentioned in Chapter 3, a new higher value of resonant frequency chosen because the switching frequency used in wireless power transfer is higher which is up to 100 kHz. In order to get more ideal value of resonant frequency, the resonant frequency is changed from 55 kHz to 90 kHz. The characteristics of the output waveform that is produced from the RC circuit with $F_r = 90$ kHz is observed. The basic RC circuit is shown below.



When $F_s = 100 \text{ kHz}$;

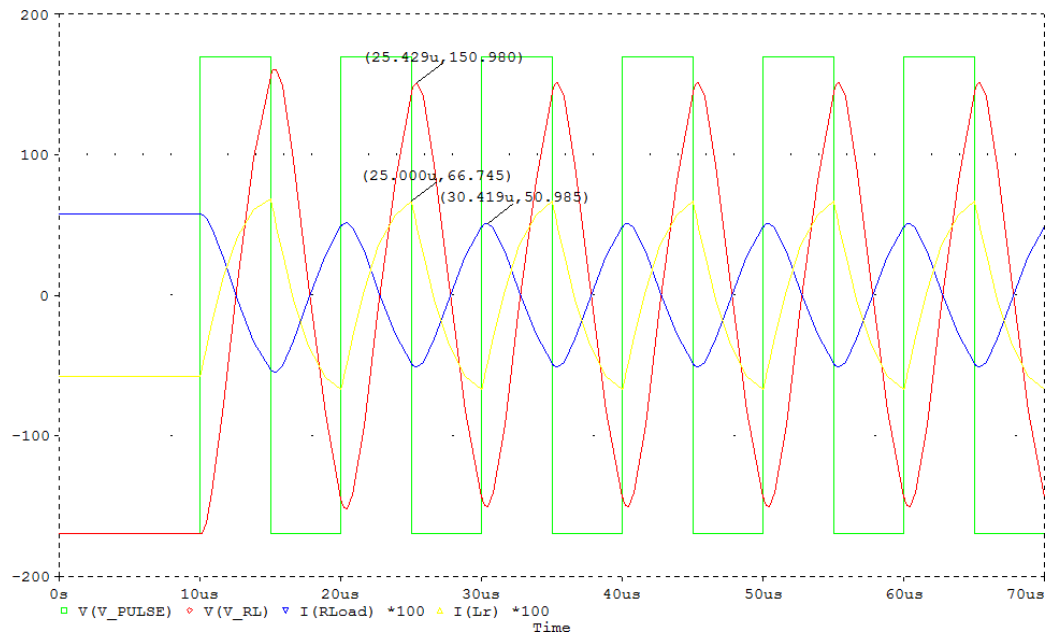


Figure 16: Voltage and Current Waveform for $F_s = 100\text{kHz}$

When $F_s = 110 \text{ kHz}$;

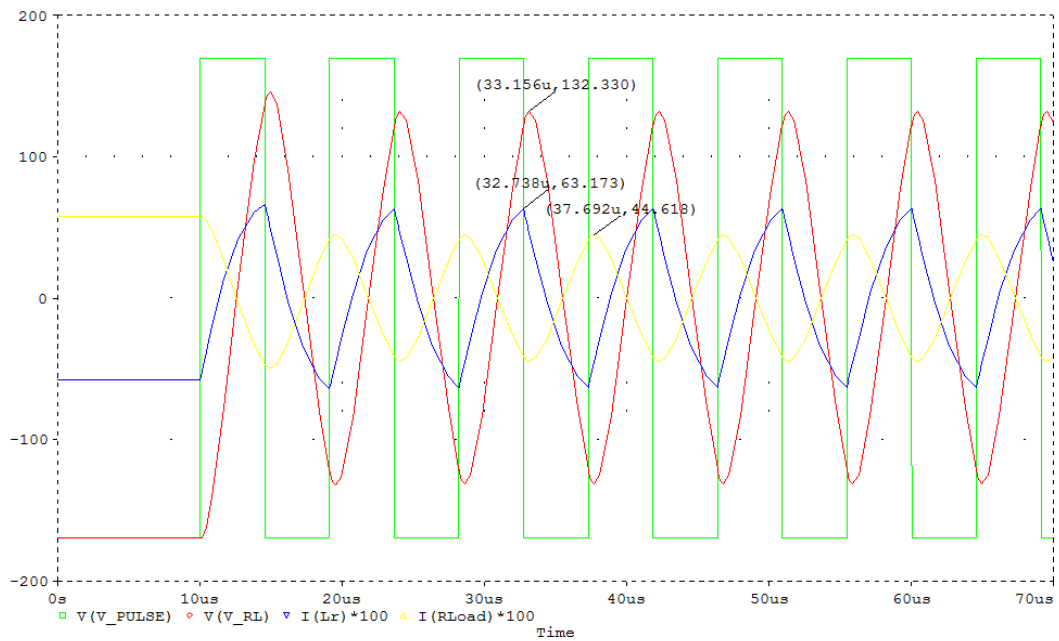


Figure 17: Voltage and Current Waveform for $F_s = 110\text{kHz}$

When $F_s = 120 \text{ kHz}$;

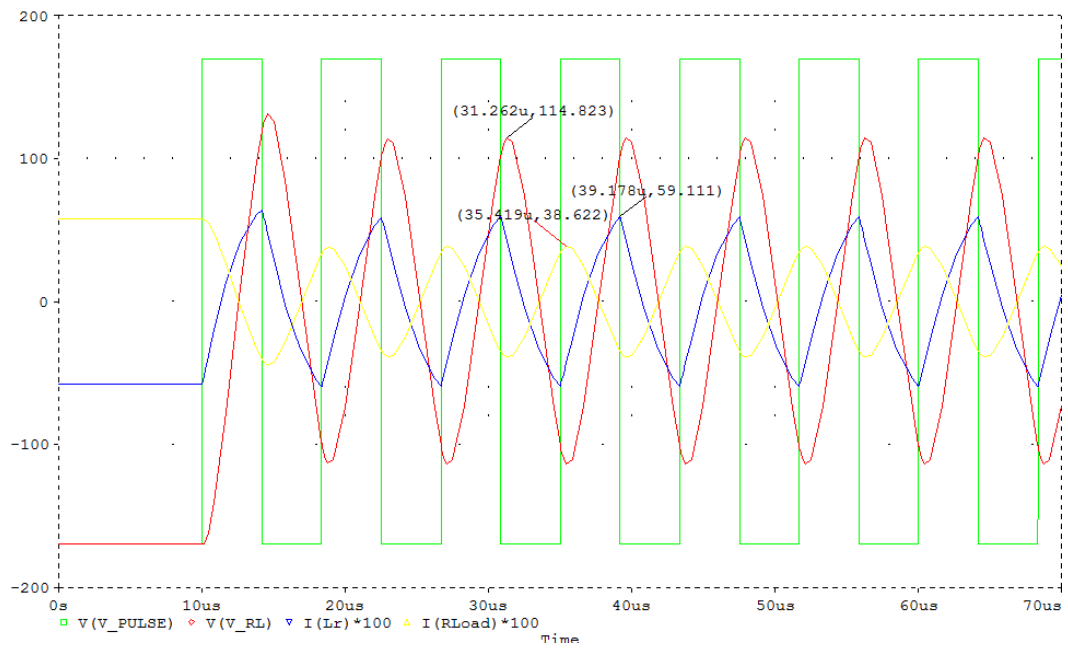


Figure 18: Voltage and Current Waveform for $F_s = 120 \text{ kHz}$

When $F_s = 130 \text{ kHz}$;

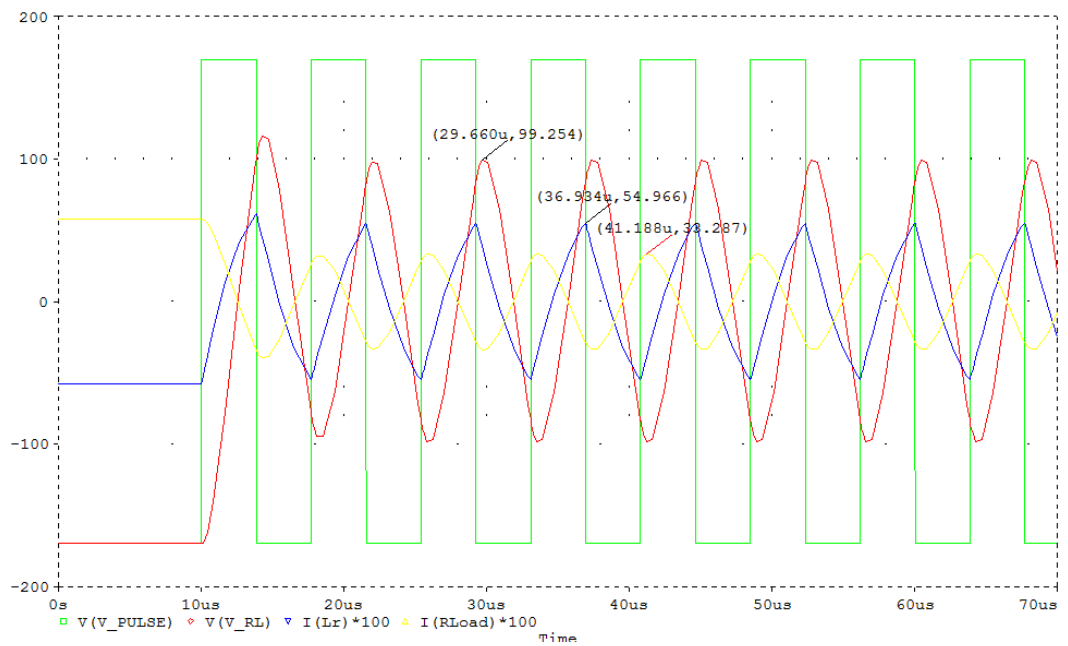


Figure 19: Voltage and Current Waveform for $F_s = 130 \text{ kHz}$

When $F_s = 140 \text{ kHz}$;

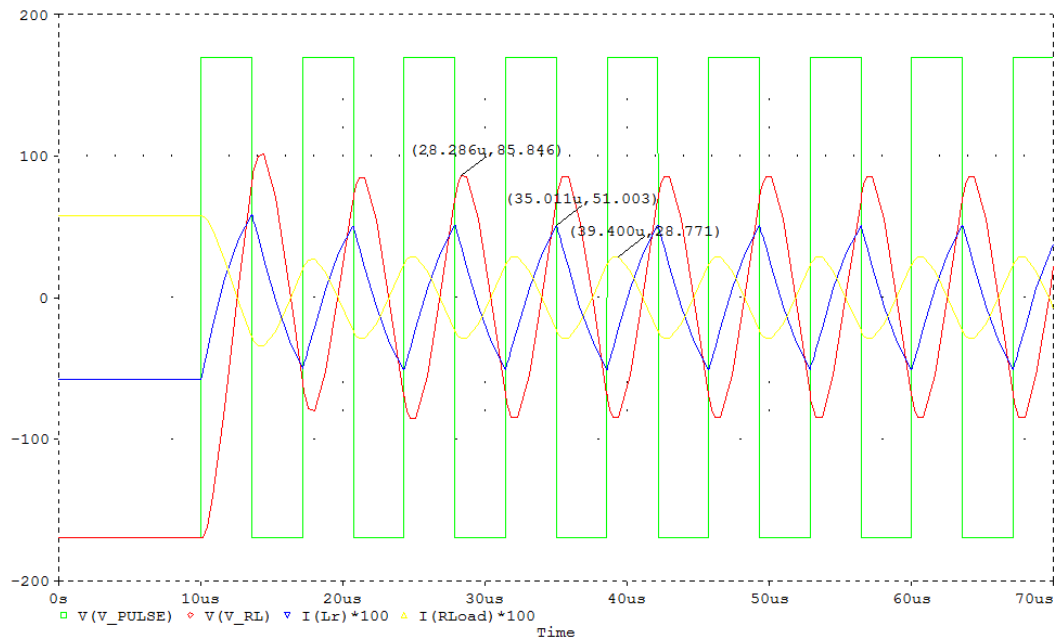


Figure 20: Voltage and Current Waveform for $F_s = 140 \text{ kHz}$

When $F_s = 150 \text{ kHz}$;

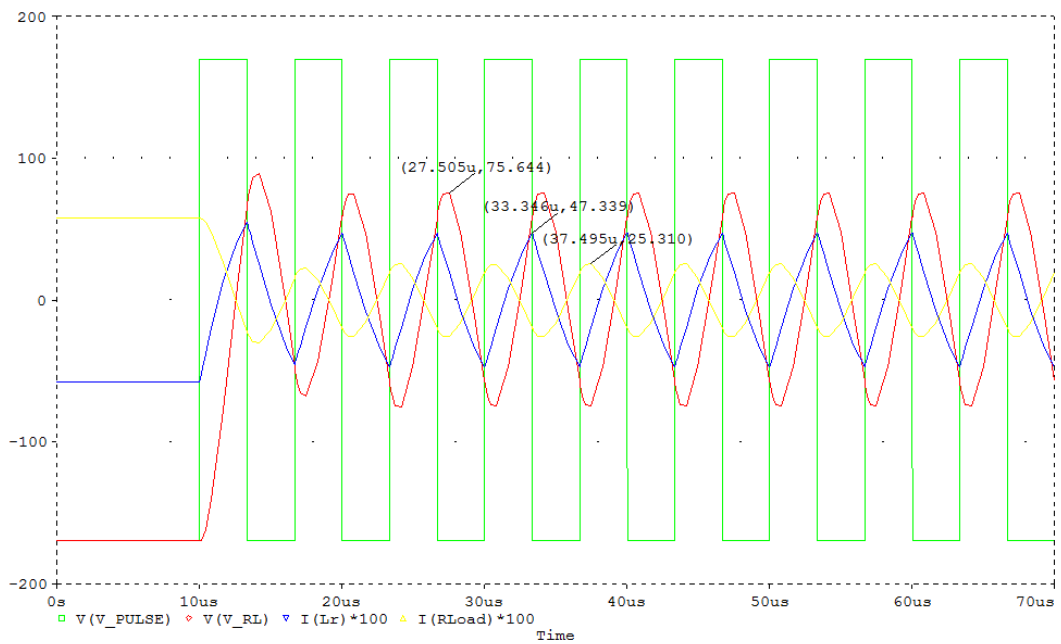


Figure 21: Voltage and Current Waveform for $F_s = 150 \text{ kHz}$

When $F_s = 160 \text{ kHz}$;

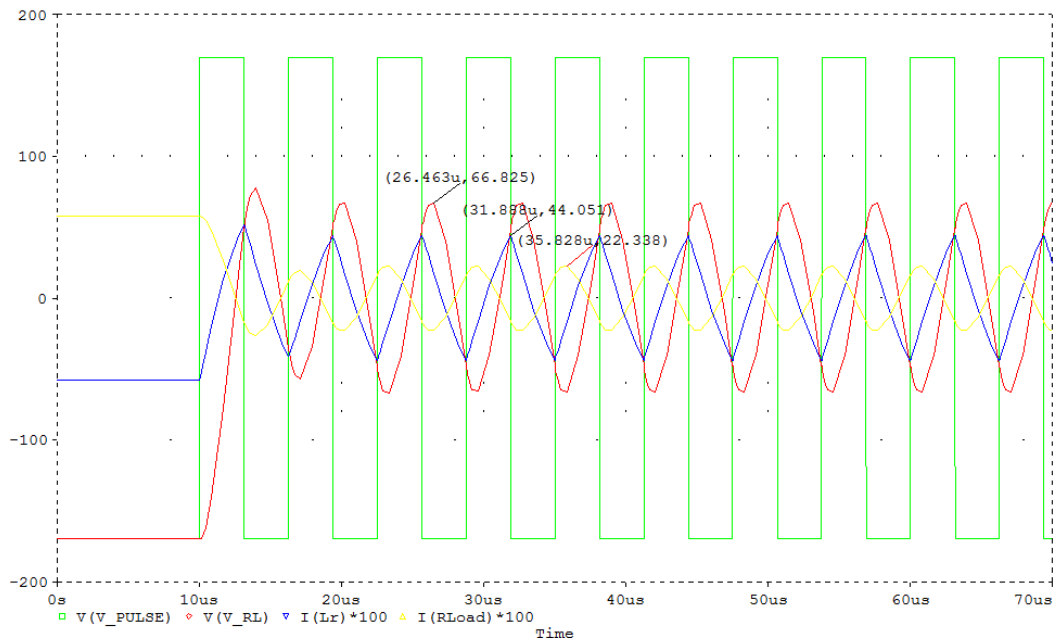


Figure 22: Voltage and Current Waveform for $F_s = 160\text{kHz}$

When $F_s = 170 \text{ kHz}$;

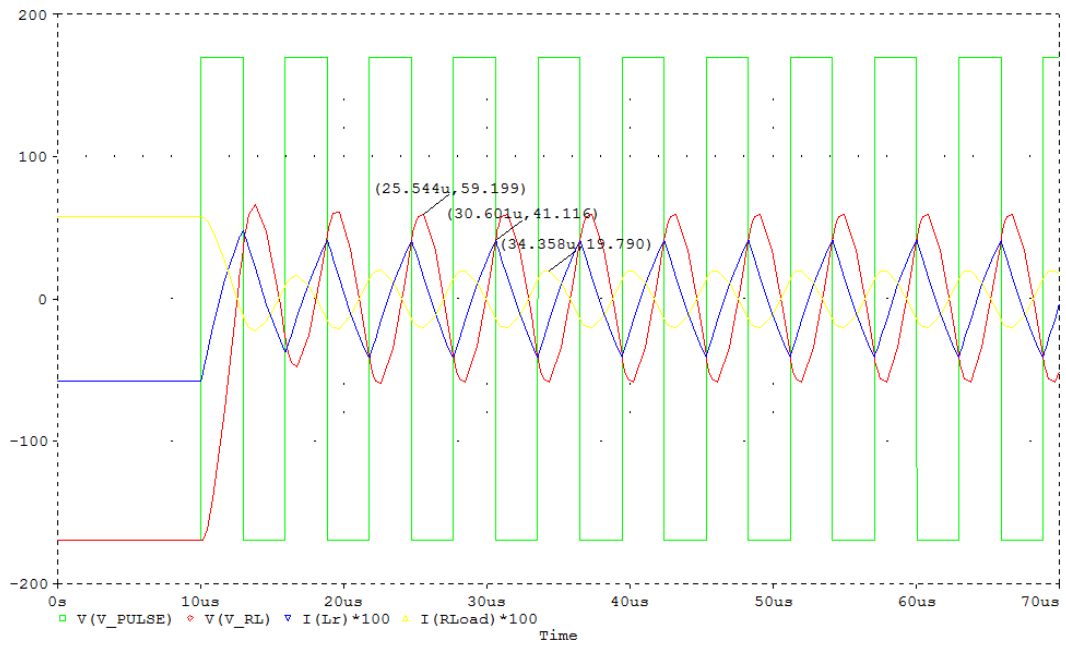


Figure 23: Voltage and Current Waveform for $F_s = 170\text{kHz}$

When $F_s = 180 \text{ kHz}$;

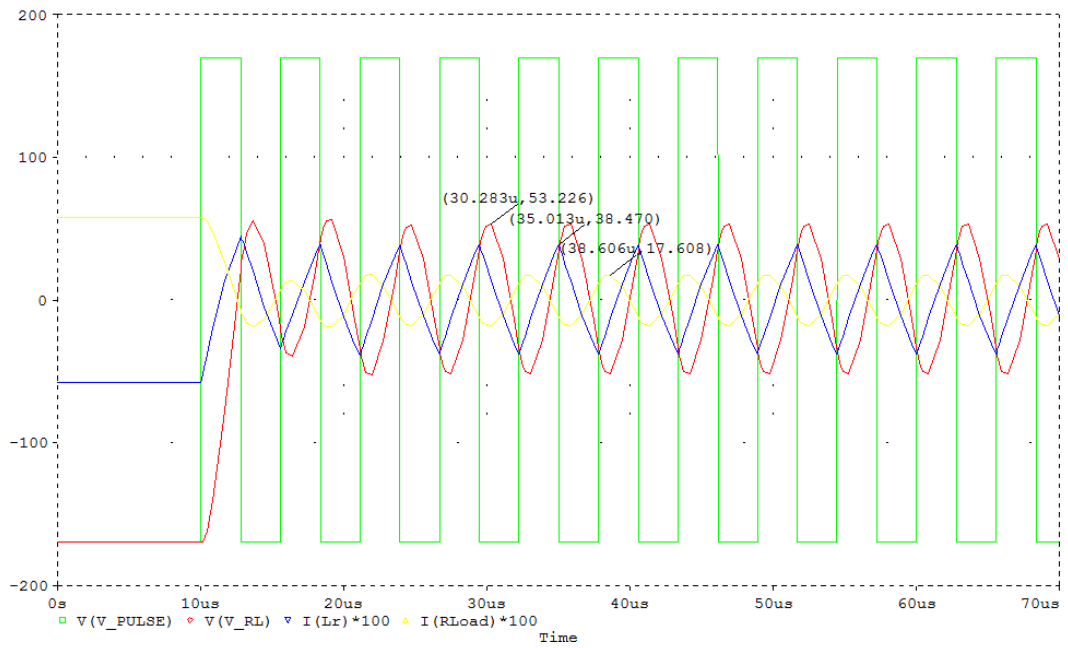


Figure 24: Voltage and Current Waveform for $F_s = 180\text{kHz}$

When $F_s = 190 \text{ kHz}$;

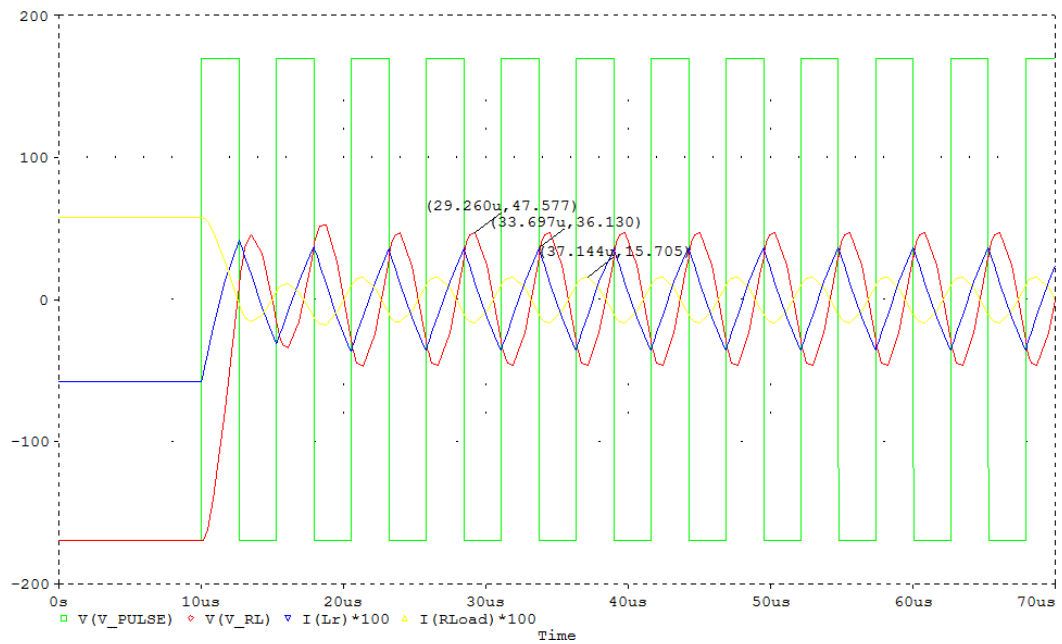


Figure 25: Voltage and Current Waveform for $F_s = 190\text{kHz}$

When $F_s = 200 \text{ kHz}$;

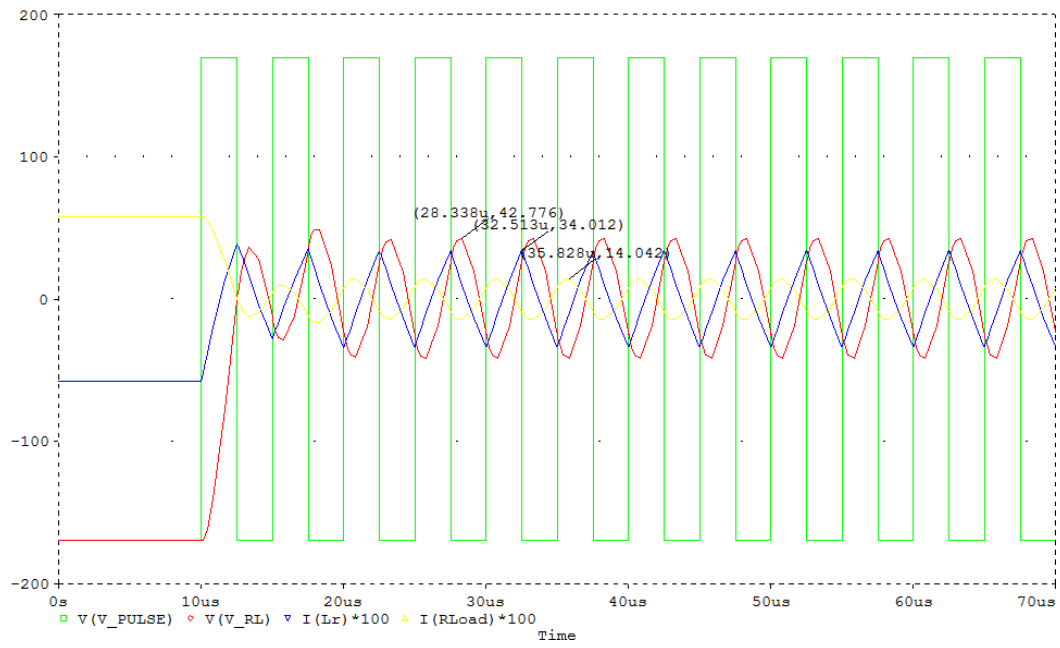


Figure 26: Voltage and Current Waveform for $F_s = 200\text{kHz}$

When $F_s = 210 \text{ kHz}$;

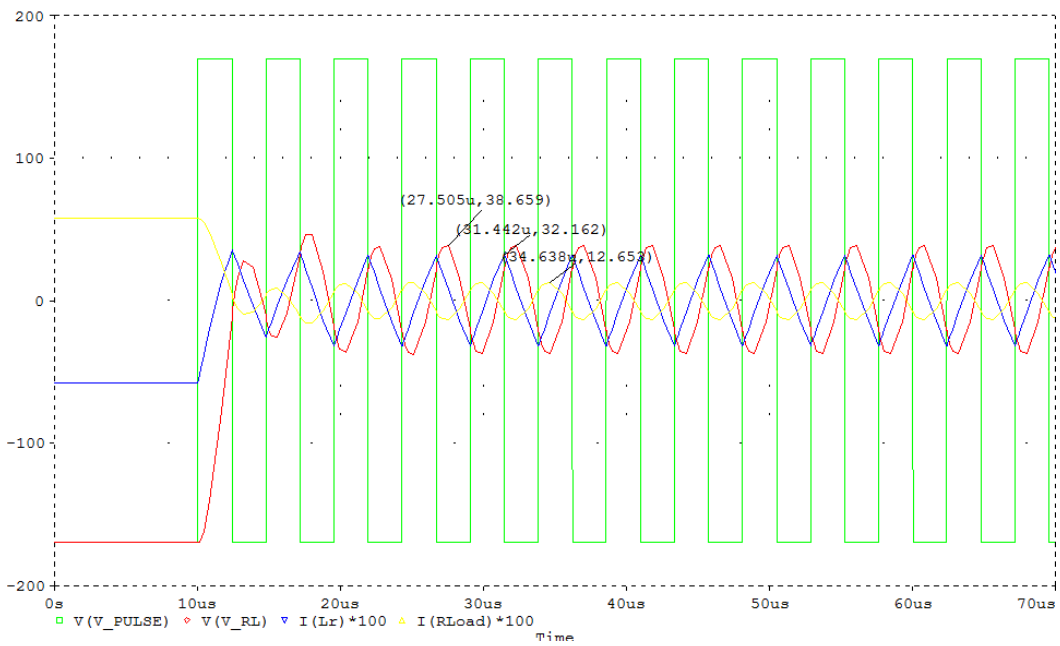


Figure 27: Voltage and Current Waveform for $F_s = 210\text{kHz}$

When $F_s = 220 \text{ kHz}$;

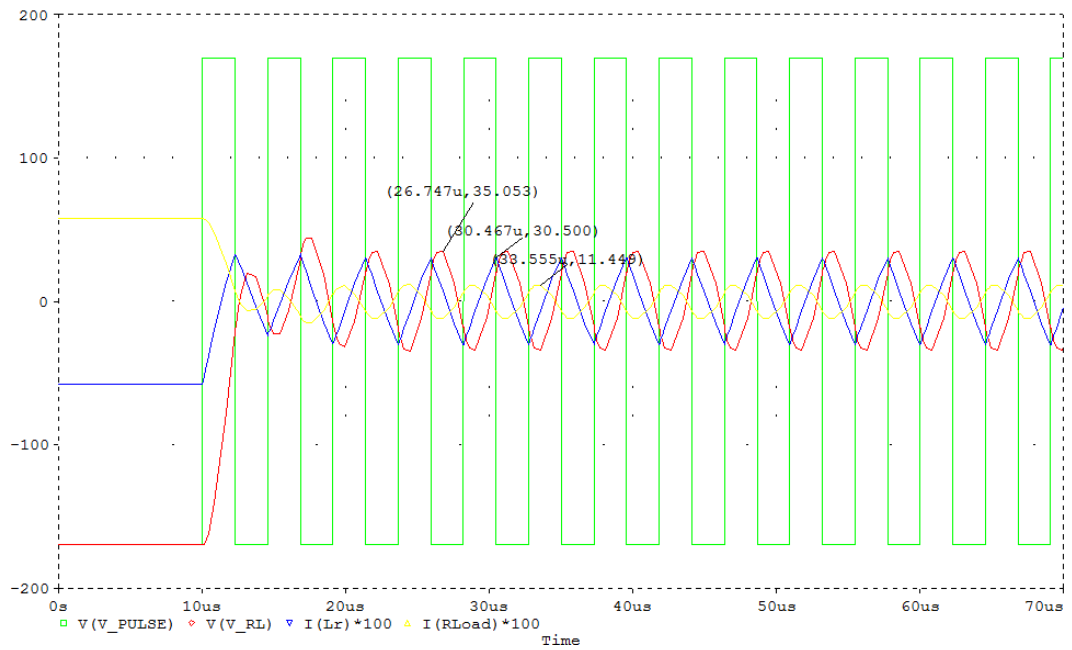


Figure 28: Voltage and Current Waveform for $F_s = 220\text{kHz}$

When $F_s = 230 \text{ kHz}$;

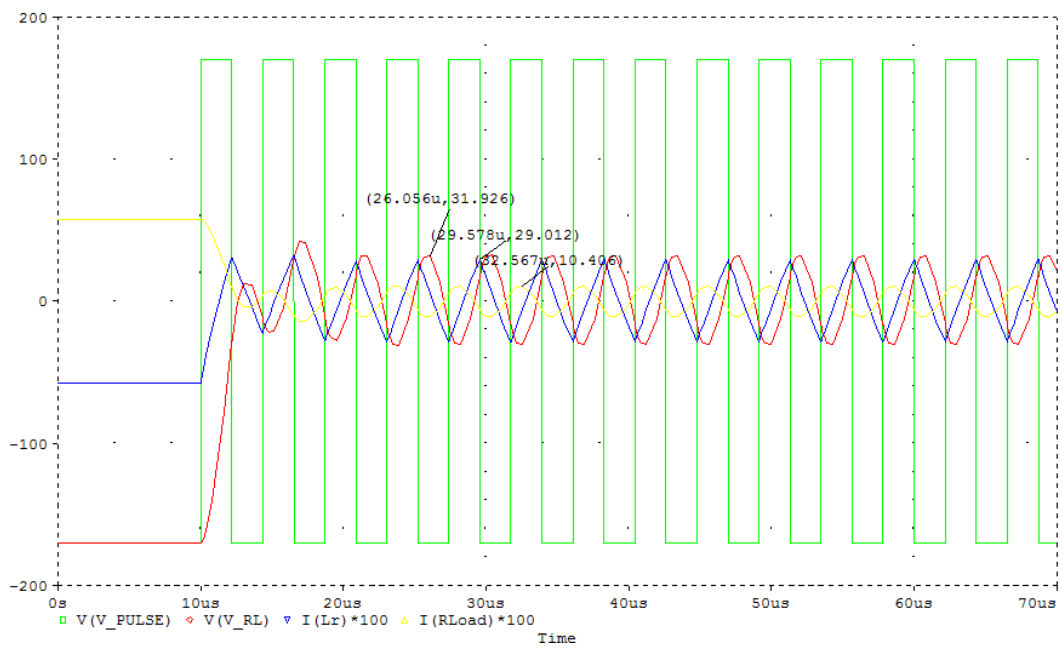


Figure 29: Voltage and Current Waveform for $F_s = 230\text{kHz}$

When $F_s = 240 \text{ kHz}$;

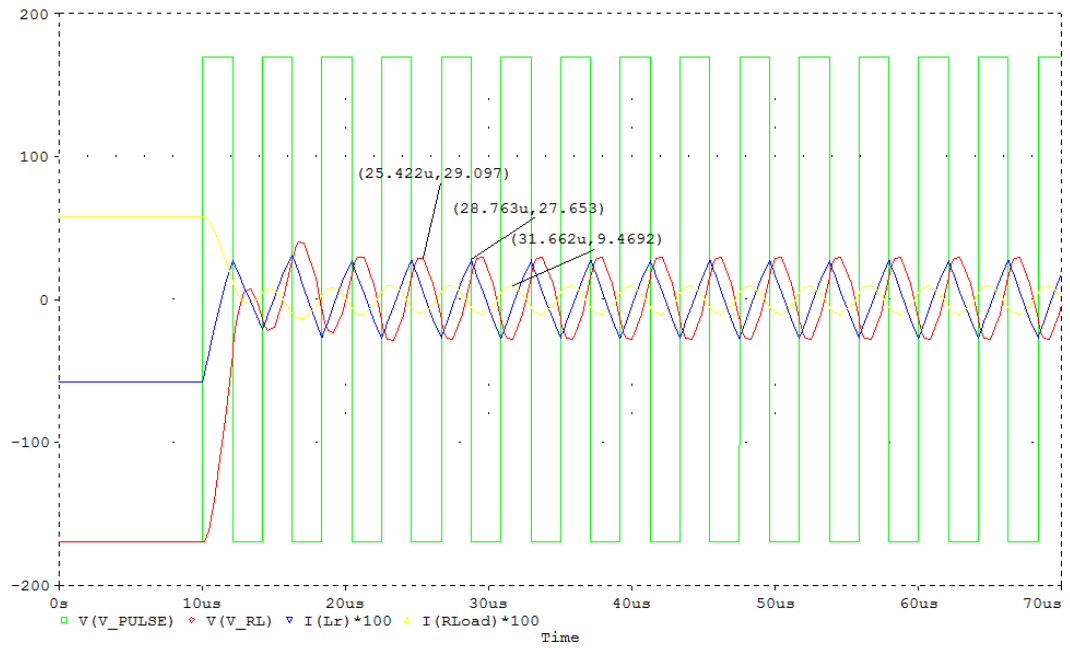


Figure 30: Voltage and Current Waveform for $F_s = 240 \text{ kHz}$

When $F_s = 250 \text{ kHz}$;

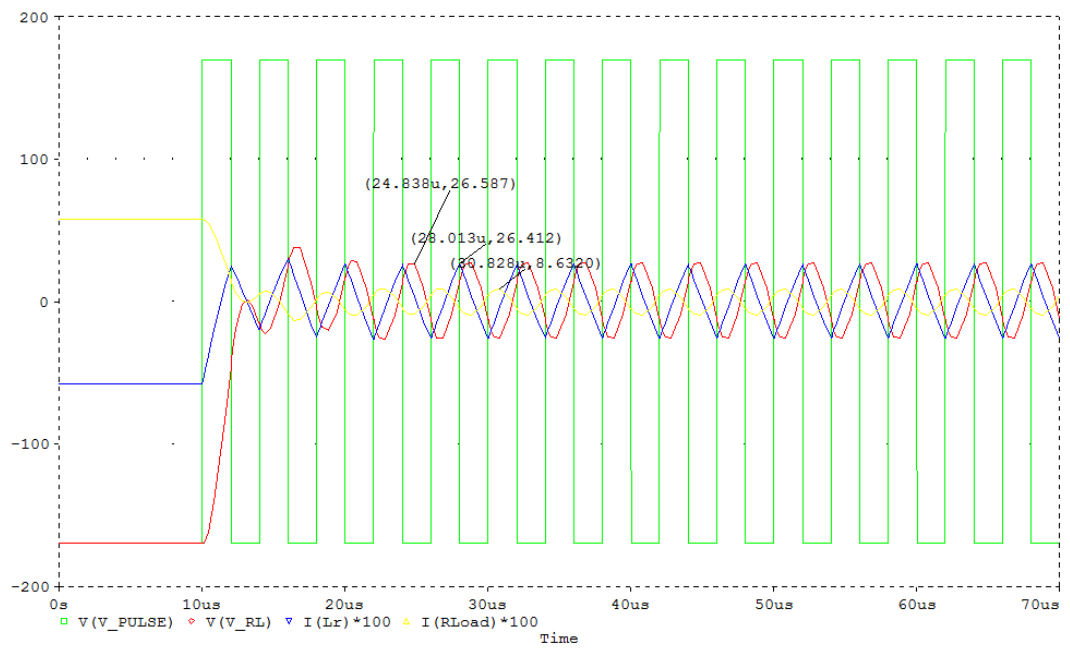


Figure 31: Voltage and Current Waveform for $F_s = 250 \text{ kHz}$

When $F_s = 260 \text{ kHz}$;

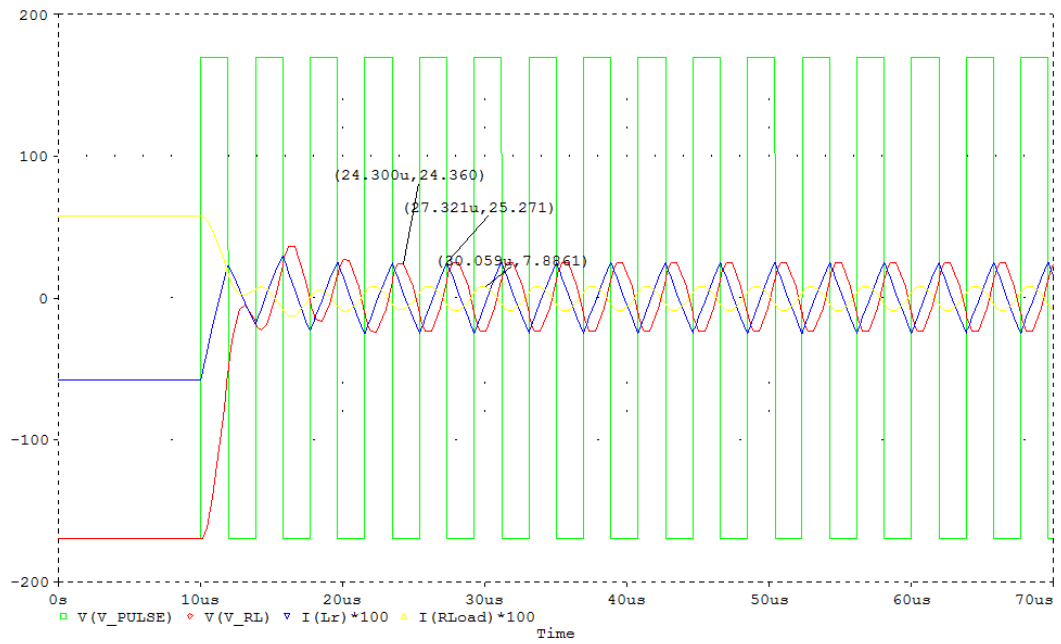


Figure 32: Voltage and Current Waveform for $F_s = 260\text{kHz}$

When $F_s = 270 \text{ kHz}$;

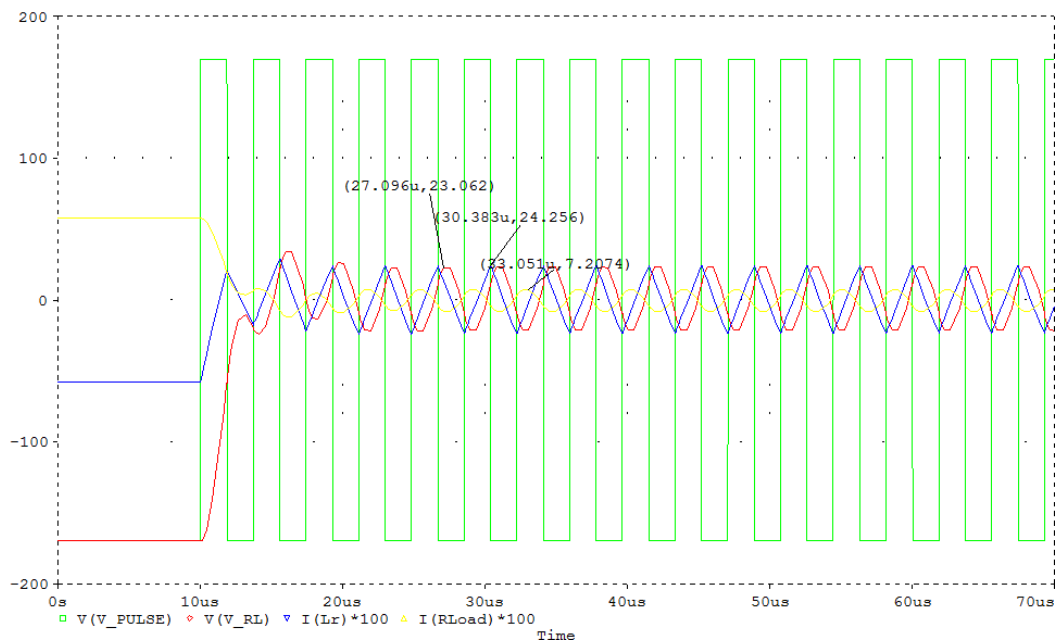


Figure 33: Voltage and Current Waveform for $F_s = 270\text{kHz}$

When $F_s = 280 \text{ kHz}$;

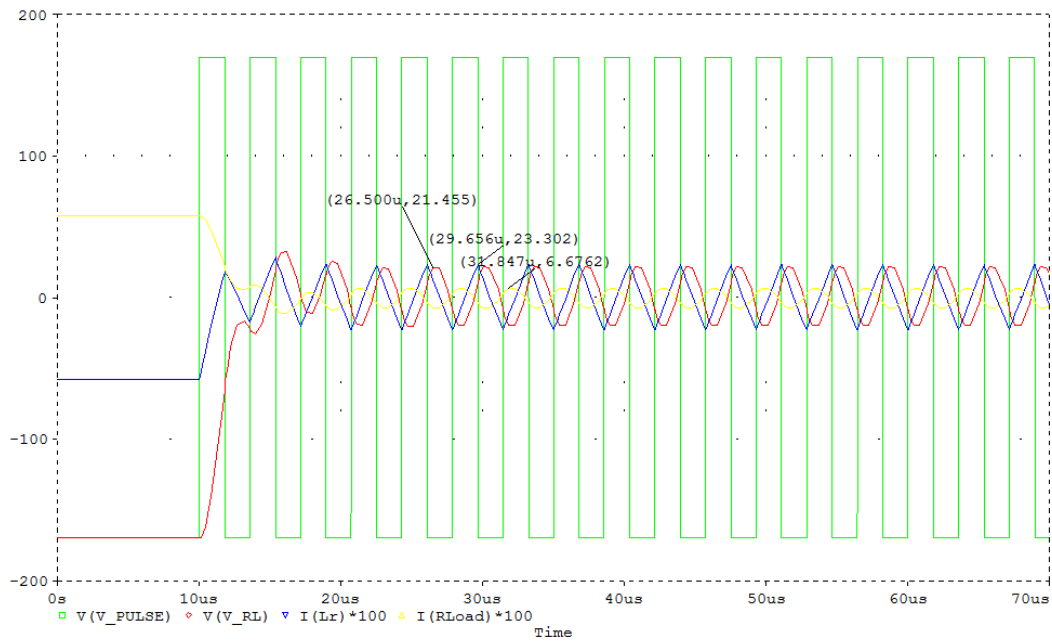


Figure 34: Voltage and Current Waveform for $F_s = 280\text{kHz}$

The values of the current and voltage at the load and the current at the inductor for RC circuit with $F_r = 90 \text{ kHz}$ are tabulate in the table below :

No.	Frequency (kHz)	V_R (V)	I_R (A)	I_L (A)	
				PEAK	RMS
1	90	170.0050	0.5746	0.6896	0.4876
2	100	150.9800	0.5099	0.6675	0.4720
3	110	132.3300	0.4462	0.6317	0.4467
4	120	114.8230	0.3862	0.5911	0.4180
5	130	99.2540	0.3329	0.5497	0.3887
6	140	85.8460	0.2877	0.5100	0.3606
7	150	75.6440	0.2531	0.4734	0.3347
8	160	66.8250	0.2234	0.4405	0.3115
9	170	59.1990	0.1979	0.4112	0.2907
10	180	53.2260	0.1760	0.3847	0.2720
11	190	47.5770	0.1571	0.3613	0.2555

12	200	42.7760	0.1404	0.3401	0.2405
13	210	38.6590	0.1265	0.3216	0.2274
14	220	35.0530	0.1145	0.3050	0.2157
15	230	31.9260	0.1041	0.2901	0.2051
16	240	29.0970	0.0947	0.2765	0.1955
17	250	26.5870	0.0863	0.2641	0.1868
18	260	24.3600	0.0789	0.2527	0.1787
19	270	23.0620	0.0721	0.2426	0.1715
20	280	21.4550	0.0668	0.2303	0.1629

Table 5: Parameters with different switching frequency for $F_r = 90$ kHz

Based on the data tabulated in Table 5, the values of the important parameters at the load and at the inductor are plotted as shown below:

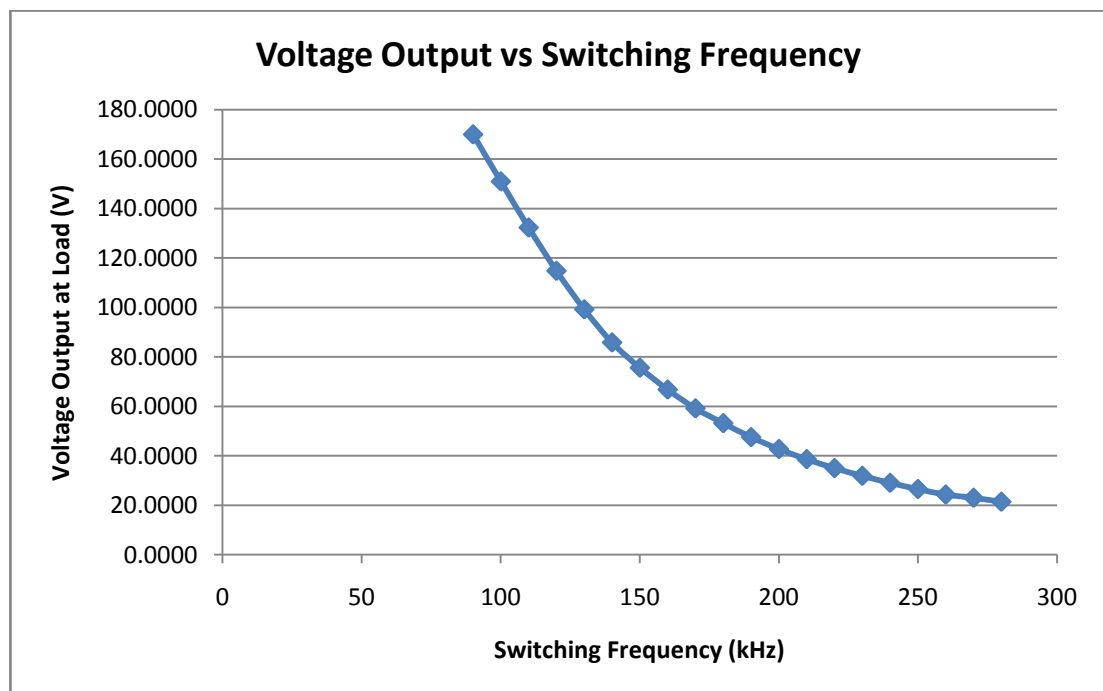


Figure 35: Voltage output vs switching frequency ($F_r=90$ kHz)

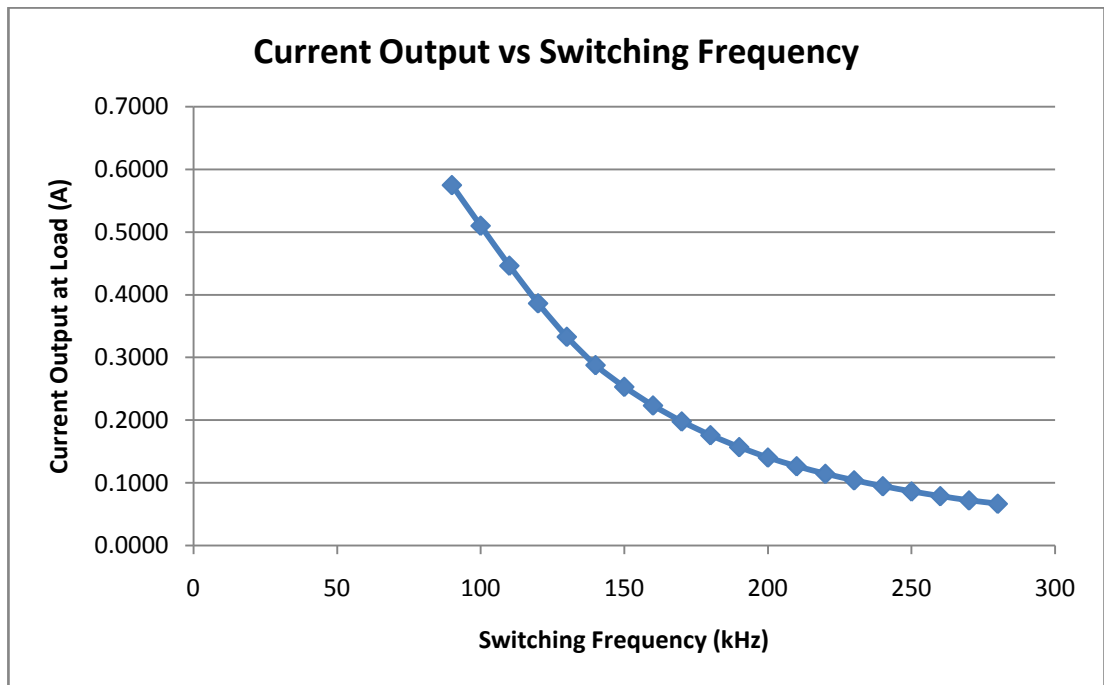


Figure 36: Current output vs switching frequency ($F_r=90\text{kHz}$)

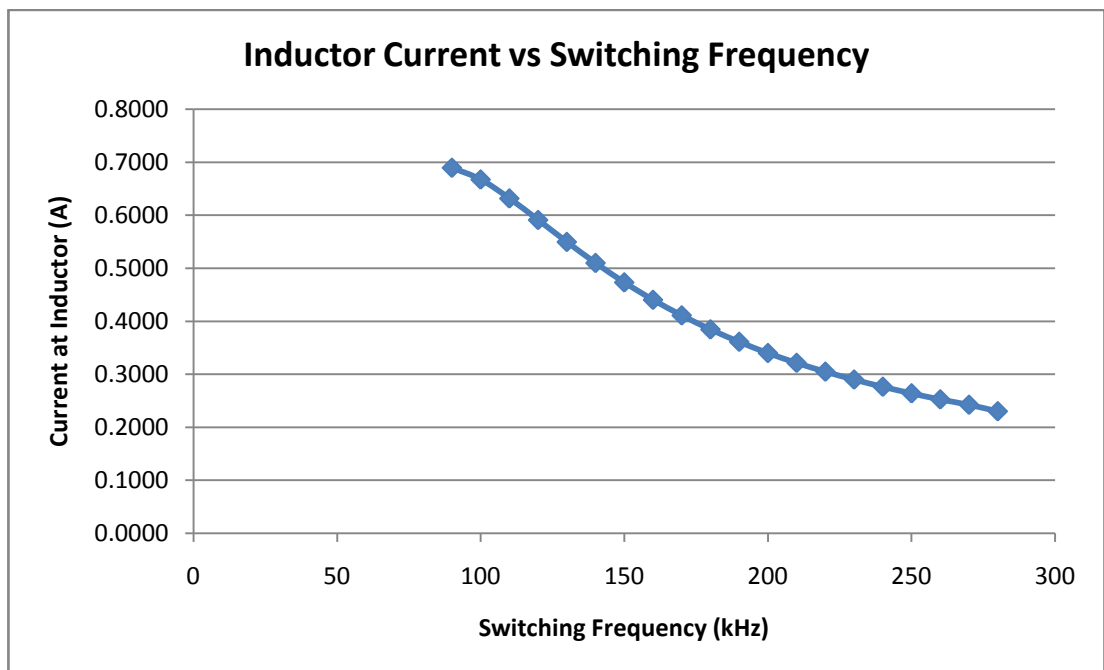
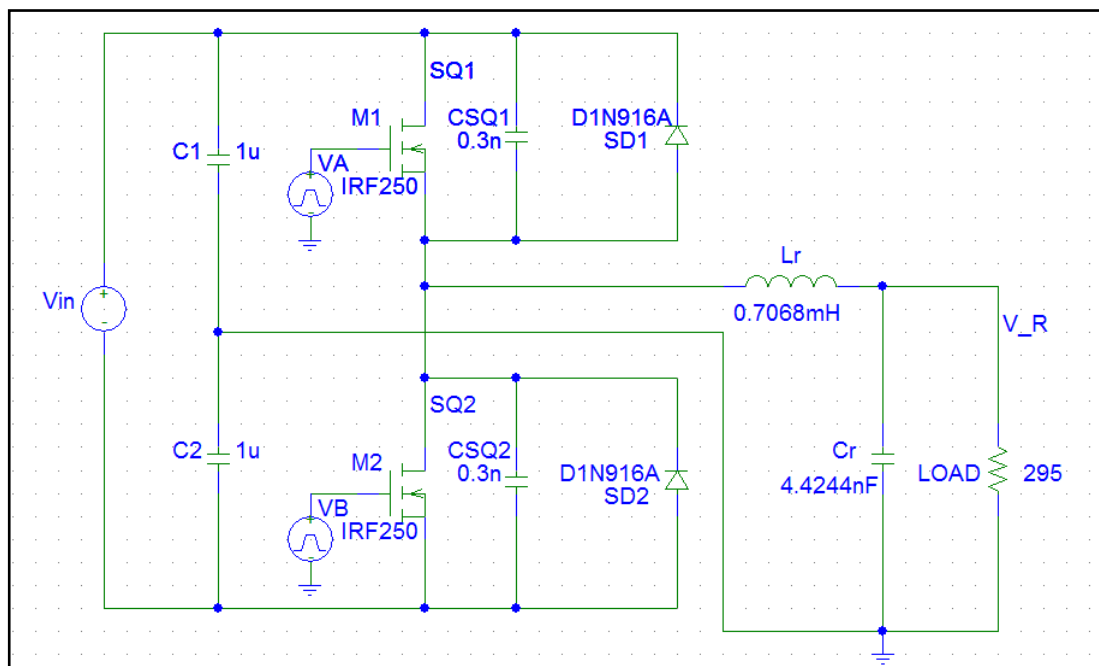


Figure 37: Inductor current vs switching frequency ($F_r=90\text{kHz}$)

Because of higher switching frequency to be used in the wireless power transfer, a decision to change the previous resonant frequency of 55 kHz to 90 kHz has been made and the characteristics of the output voltage when using $f_r=90\text{ kHz}$ is analyzed. The output voltage and output current at the load is decreasing as the switching frequency applied is increasing. That mean the output voltage of the circuit can be controlled by adjusting the value of switching frequency. This is desirable because in the electric vehicle battery charging system, a variable DC voltage will be needed since the value of battery voltage which will be at the load will be different from times to times according to value of battery discharged.

4.2 Results and Discussion for Half-bridge PRC

RC circuit expanded becoming half-bridge PRC circuit gives several waveforms that needs to analyzed. The switching frequency of the Switch 1 and Switch 2 were set above resonant (100kHz). Below is the half-bridge PRC circuit that is used to simulate the voltage output and current output waveform.



SWITCHING SPECIFICATIONS

- **Switching specifications at Switch 1 (VA):**

$$V1 = -170V$$

$$V2 = 170V$$

$$TD = 10\mu s$$

$$TR = 10ns$$

$$TF = 10ns$$

$$PW = 4.98\mu s$$

$$PER = 10\mu s$$

- **Switching specifications at Switch 2 (VB):**

$$V1 = 170 V$$

$$V2 = -170 V$$

$$TD = 9.865 \mu s$$

$$TR = 10 ns$$

$$TF = 10 ns$$

$$PW = 5.25 \mu s$$

$$PER = 10 \mu s$$

4.2.1 Current Switching

To analyze the switching waveforms, there are 6 waveforms need to be observed which are:

- 1) $I(SQ1)$ or $ID(M1)$ - Current through Switch 1
- 2) $I(CSQ1)$ - Current through Capacitor (CSQ1)
- 3) $I(CSQ2)$ - Current through Capacitor (CSQ2)
- 4) $I(CSQ1)-I(CSQ2)$ - Current flows into Inductor (Lr)
- 5) $I(SD1)$ - Current through Diode (SD1)
- 6) $I(SD2)$ - Current through Diode (SD2)

Current Switching Waveforms:

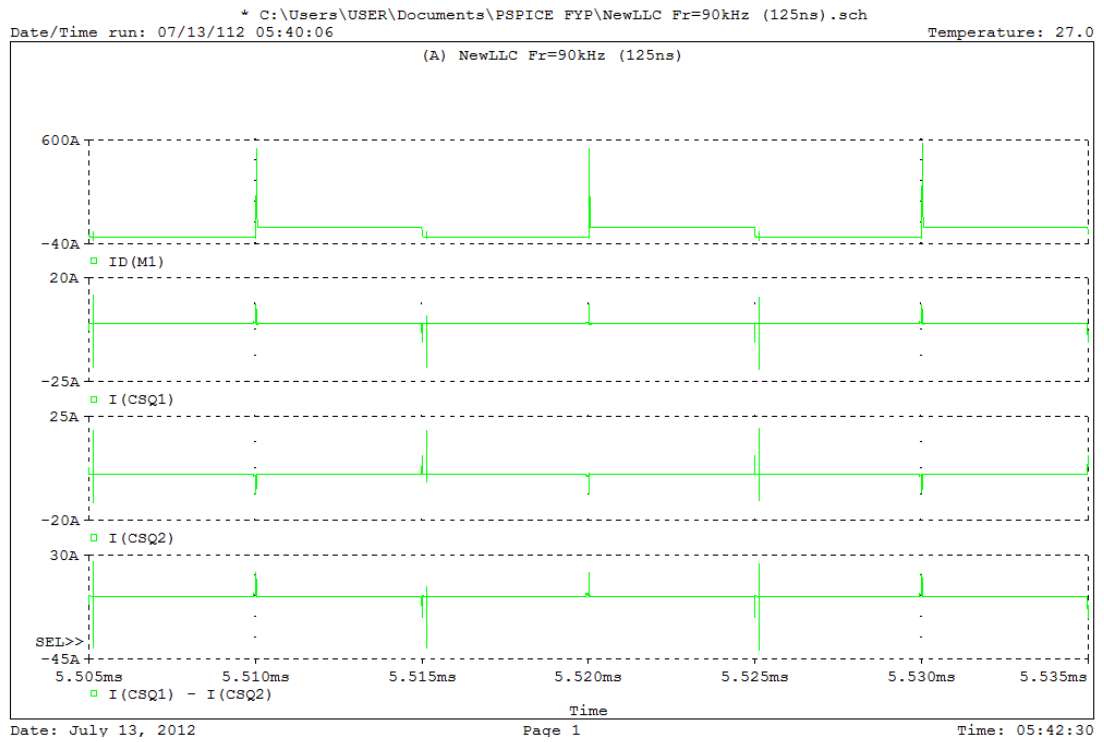


Figure 38: Waveforms of $I(D(M1))$, $I(CSQ1)$, $I(CSQ2)$ and $I(CSQ1)-I(CSQ2)$

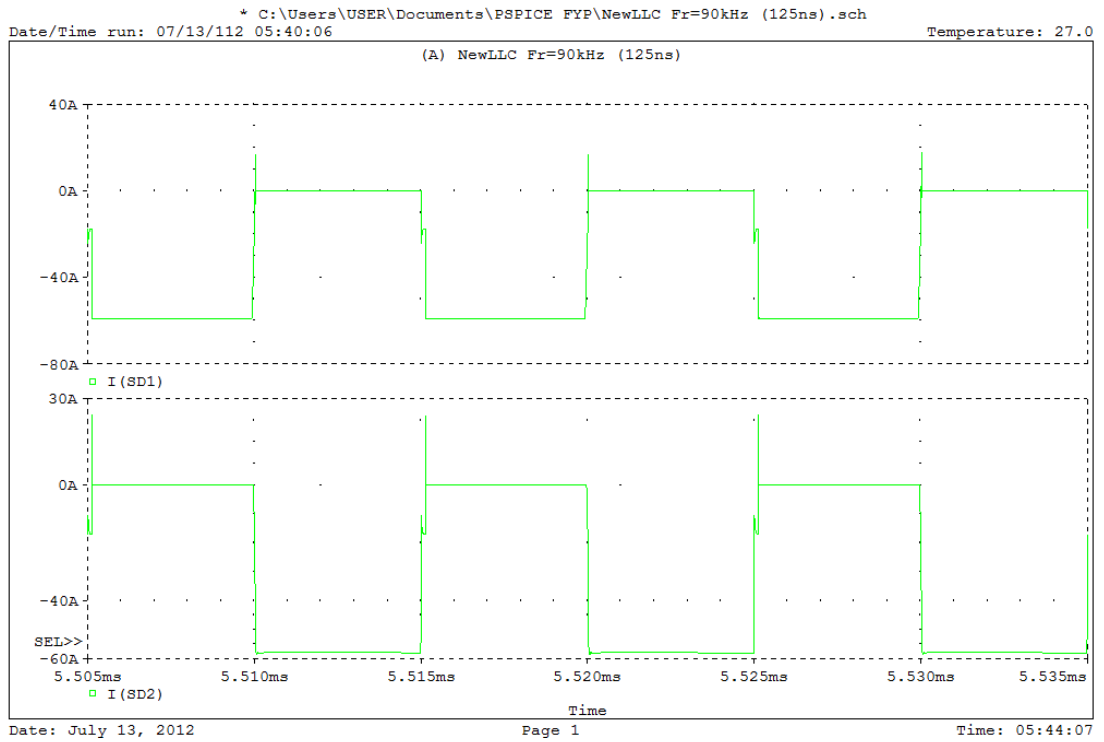


Figure 39: Waveforms of $I(SD1)$ and $I(SD2)$

4.2.2 Loseless Switching

There are six waveforms that need to be observed and analyzed to determine the loseless switching which are listed as followed:

- 1) V_A - Voltage switching frequency at Switch 1
- 2) V_B - Voltage switching frequency at Switch 2
- 3) $V(1,3)$ or $V(SQ1)$ - Voltage across power MOSFET Switch 1
- 4) $I(SQ1)$ or $ID(M1)$ - Current through Switch 1
- 5) $V(3,0)$ or $V(SQ2)$ - Voltage across power MOSFET Switch 2
- 6) $I(SQ2)$ or $ID(M2)$ - Current through Switch 2

Loseless Switching Waveforms:

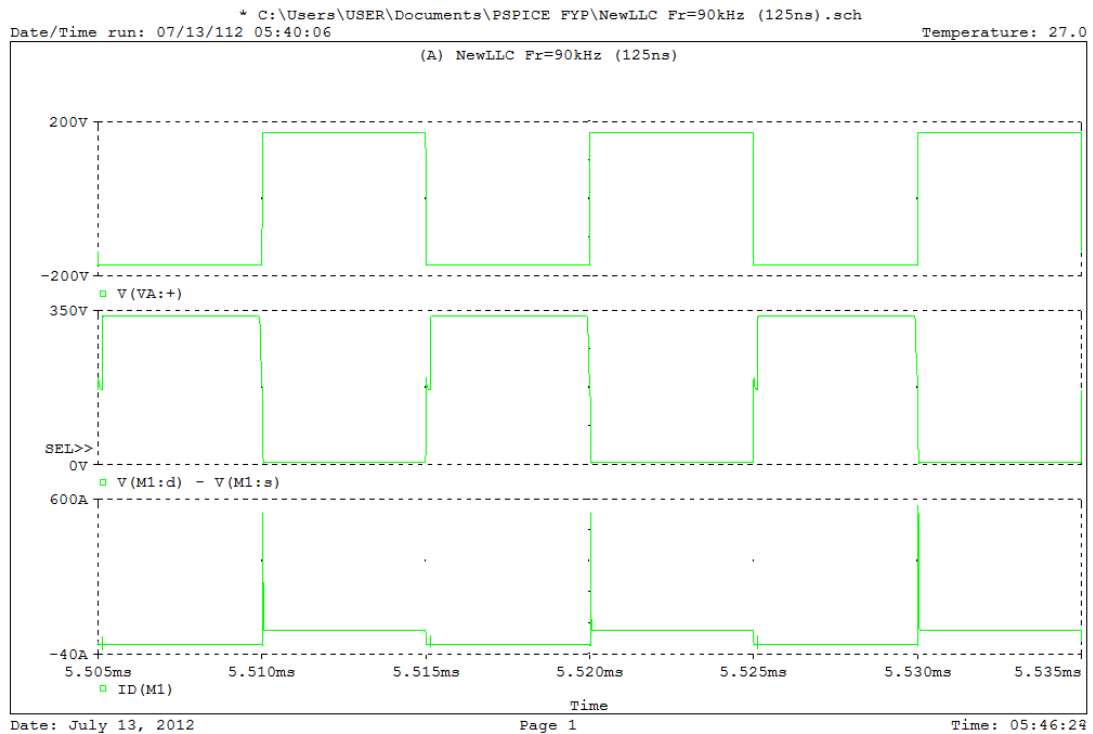


Figure 40: Waveforms of V_A , V across SQ1 and $ID(M1)$

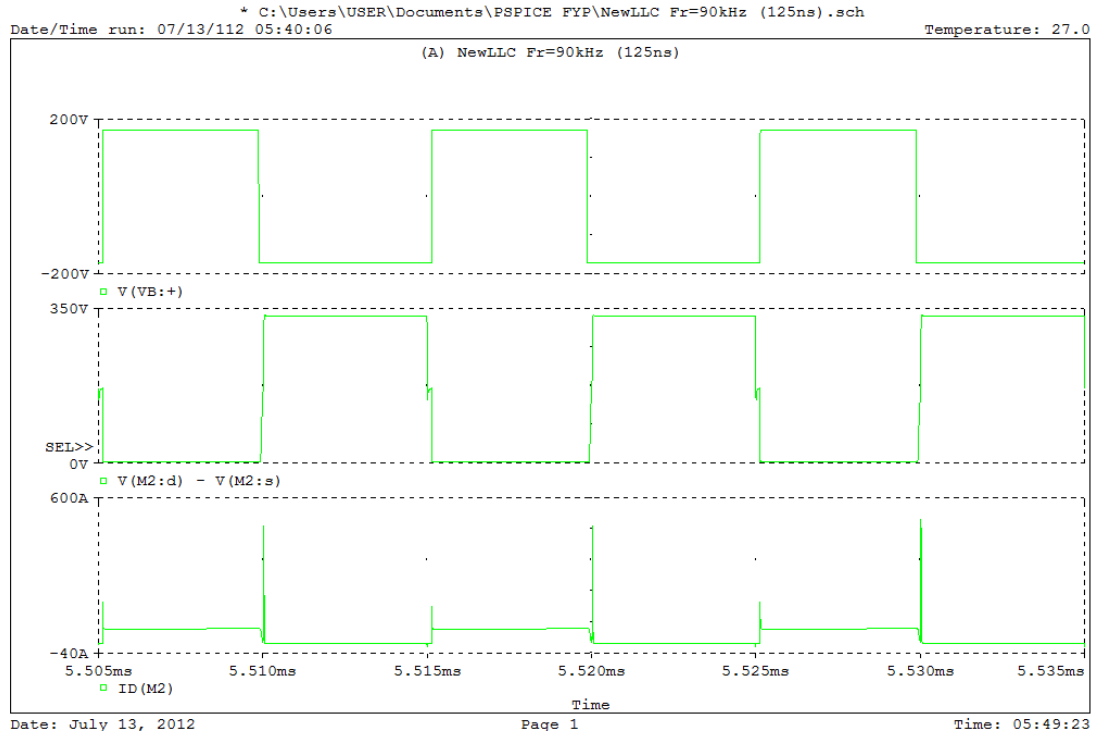


Figure 41: Waveforms of V_B , $V(SQ2)$ and $ID(M2)$

Notice that current flow through the switches will produce current spike in every transition of voltage switching frequency. This happens due to the internal resistance of the component that will result in producing current spike during the voltage transitions. However, the value of current spike 581A is minimum as compared to what we got at earlier stage of analysis which is 3.2kA. Minimum current spike means will result in a much more lower power losses at the switches.

Small value of switching losses is desirable for PRC circuit. The switching losses is determined using formula as followed:

$$\text{Switching losses, } P_S = V_{S(OFF)} \times (t_{ON} + t_{OFF}) \times I_{ON}$$

$$\text{Conduction power, } P_C = I_{ON}^2 R_{DS,ON}$$

$$\text{Total power, } P_T = P_S + P_C$$

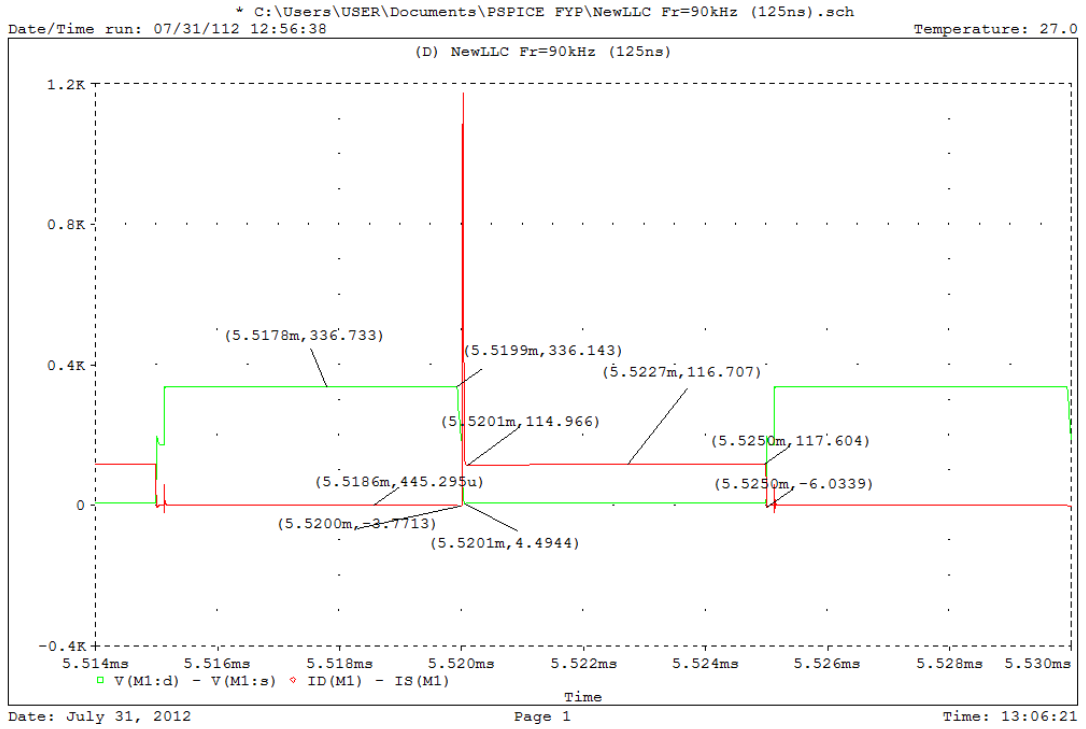


Figure 42: Switching losses at Switch A (V_A)

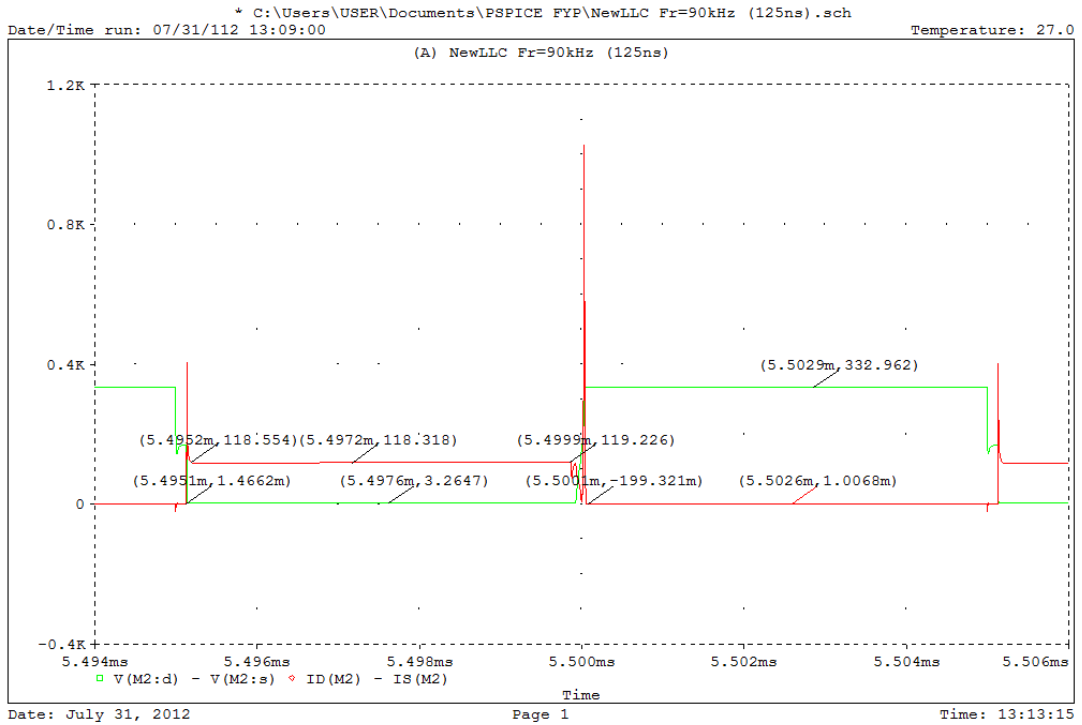


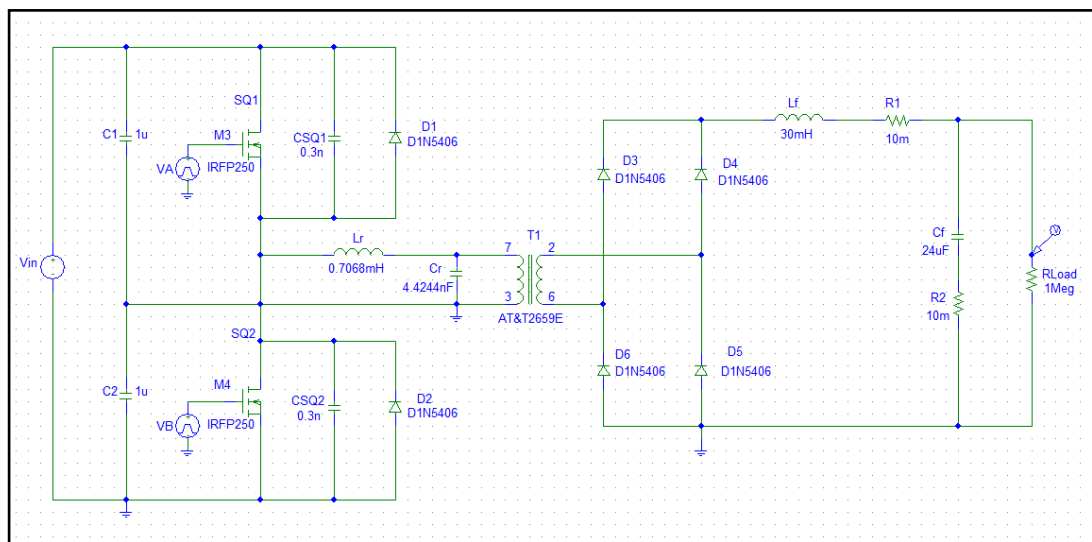
Figure 43: Switching losses at Switch B (V_B)

	Switch A	Switch B
$P_{\text{Switching}}$	10.49 W	7.73 W
$P_{\text{Conduction}}$	1.16 kW	1.19 kW
P_{Total}	1.17 kW	1.20 kW

Table 6: Switching losses and conduction losses in switch A and Switch B

As we can see in the table above, the switching losses for the switches can be considered as small. The conduction losses for both switches are also at the same rating which is 1.2 kW. This proved that the switching specification can be used in the converter design.

4.3 Results and Discussion of Converter Circuit



Output characteristics of the converter circuit needs to be analyzed. Output waveform is obtained for different values of switching frequency, F_s . The desirable output is a smooth DC voltage that will vary according to value of switching frequency. The results are as followed:

For $F_s = 100 \text{ kHz}$;

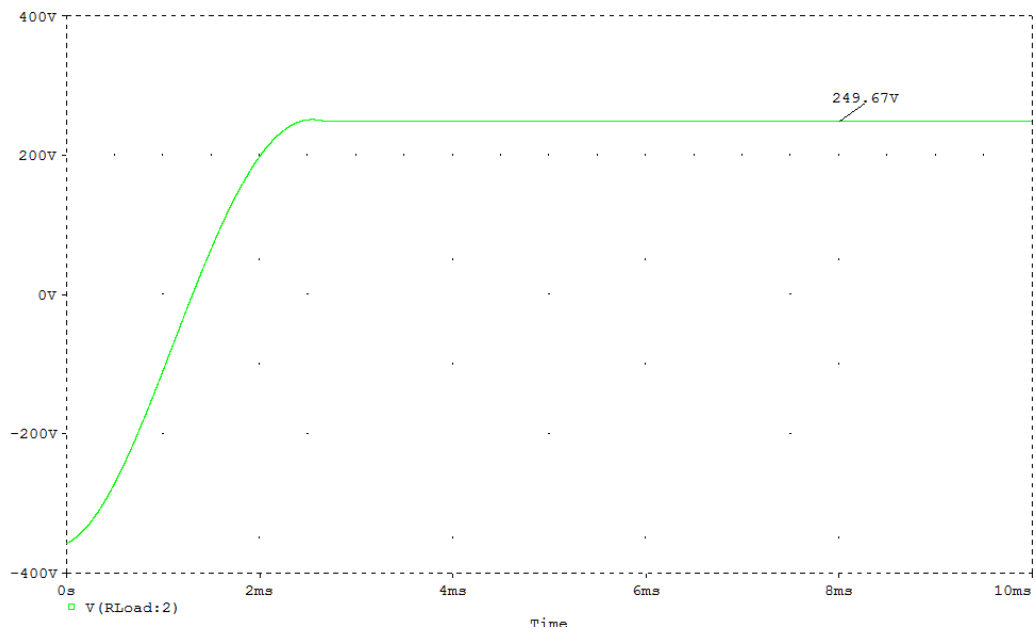


Figure 44: Converter output waveform for $F_s=100 \text{ kHz}$

For $F_s = 110 \text{ kHz}$;

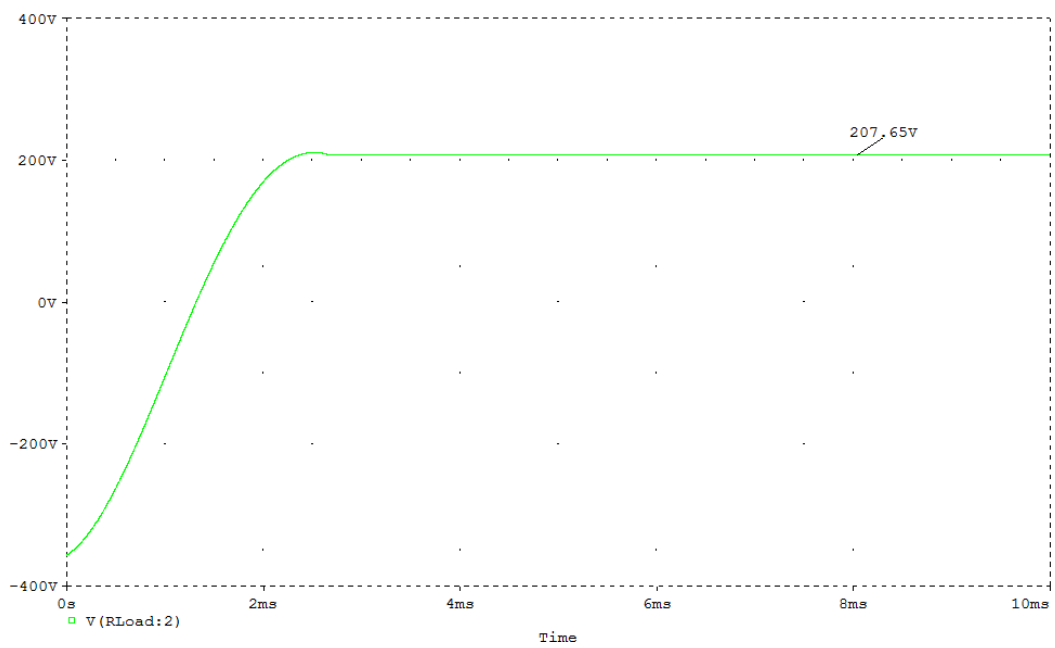


Figure 45: Converter output waveform for $F_s=110 \text{ kHz}$

For $F_s = 120 \text{ kHz}$;

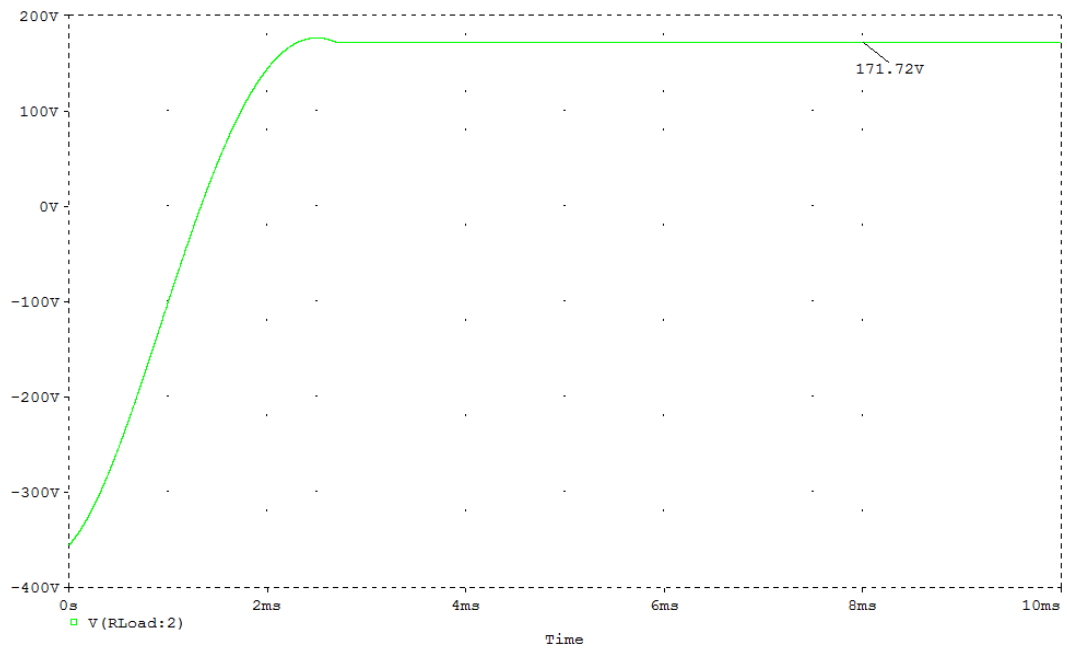


Figure 46: Converter output waveform for $F_s=120 \text{ kHz}$

For $F_s = 130 \text{ kHz}$;

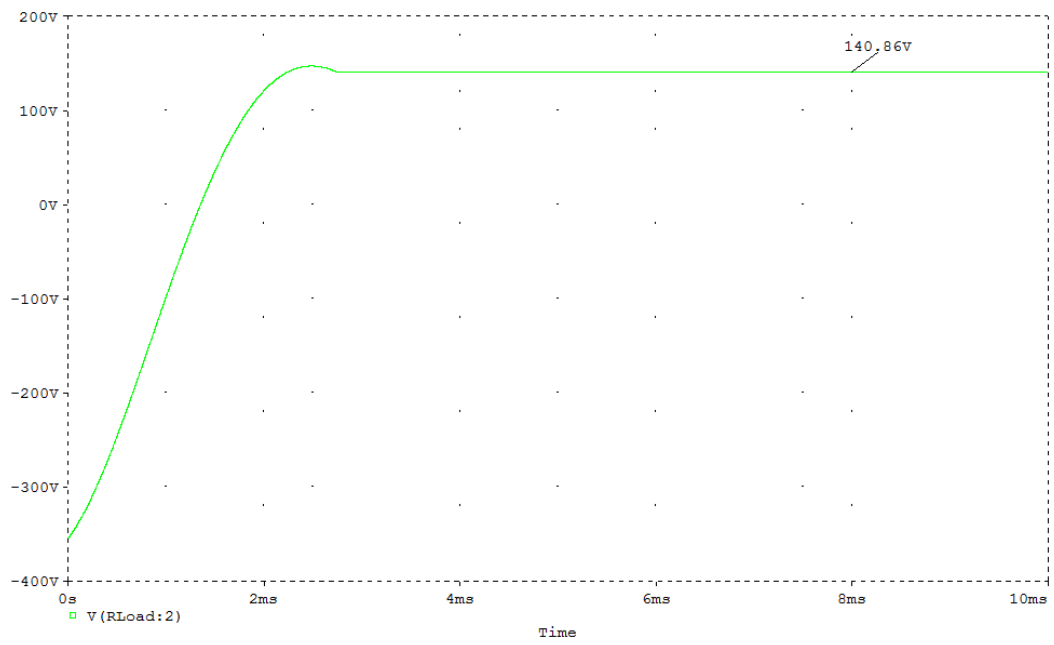


Figure 47: Converter output waveform for $F_s=130 \text{ kHz}$

For $F_s = 140 \text{ kHz}$;

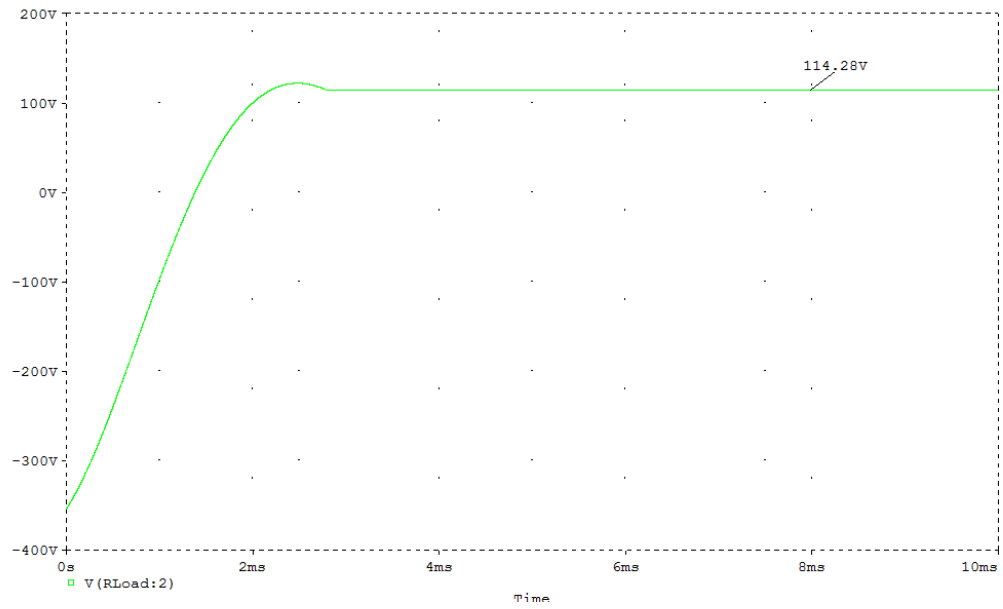


Figure 48: Converter output waveform for $F_s=140 \text{ kHz}$

For $F_s = 150 \text{ kHz}$;

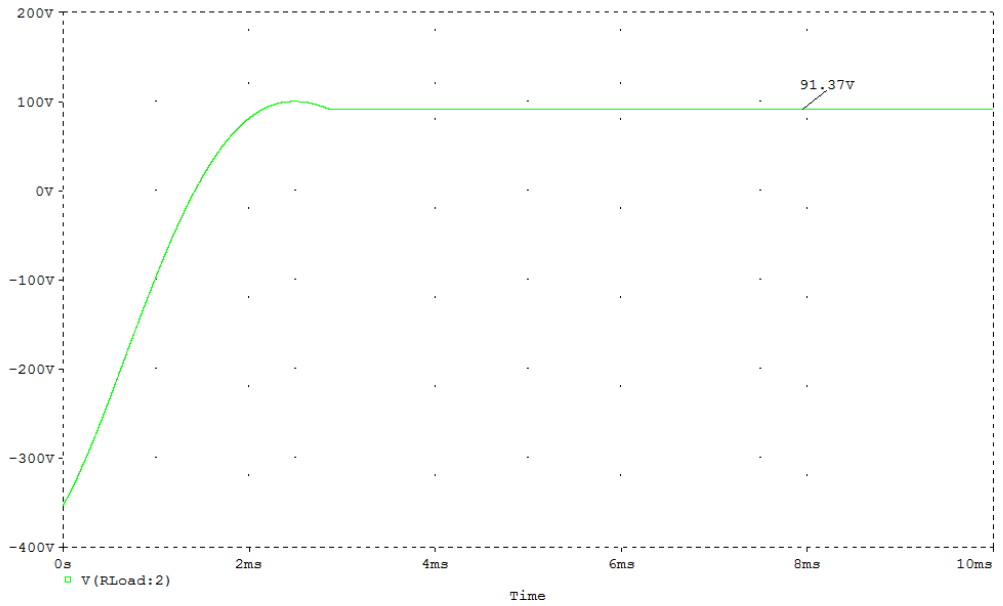


Figure 49: Converter output waveform for $F_s=150 \text{ kHz}$

For $F_s = 160 \text{ kHz}$;

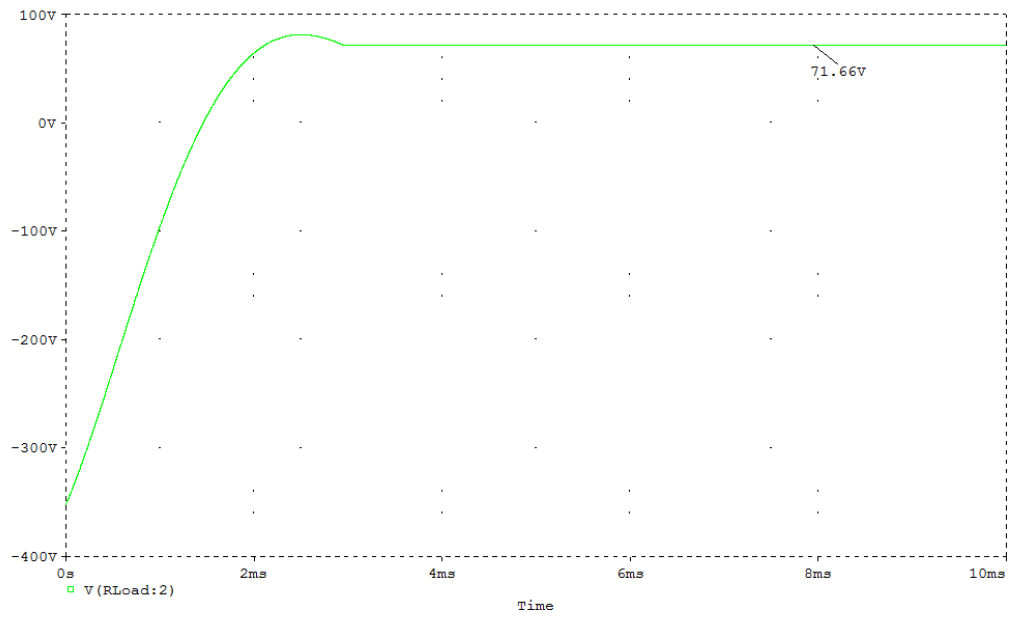


Figure 50: Converter output waveform for $F_s=160 \text{ kHz}$

For $F_s = 170 \text{ kHz}$;

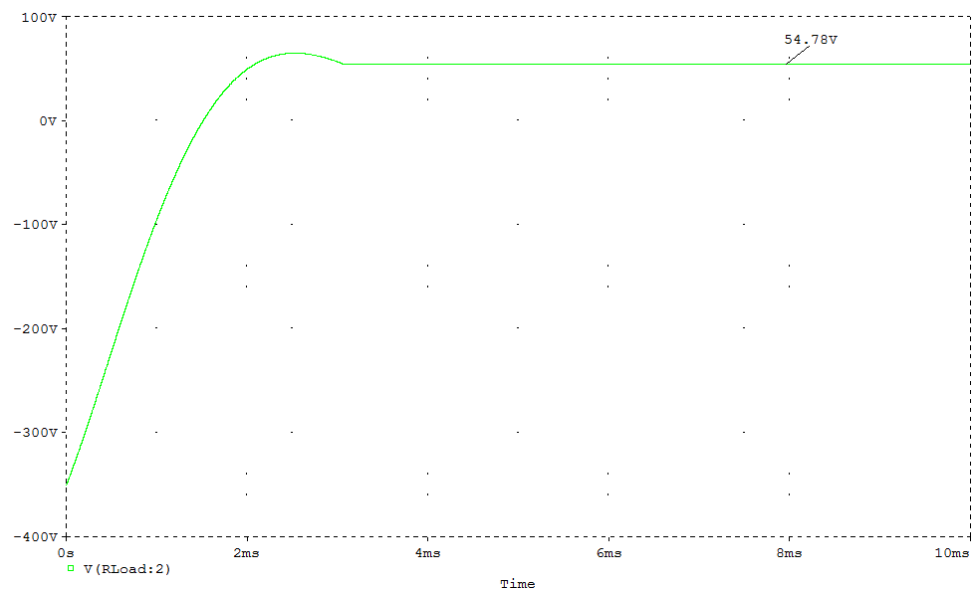


Figure 51: Converter output waveform for $F_s=170 \text{ kHz}$

For $F_s = 180 \text{ kHz}$;

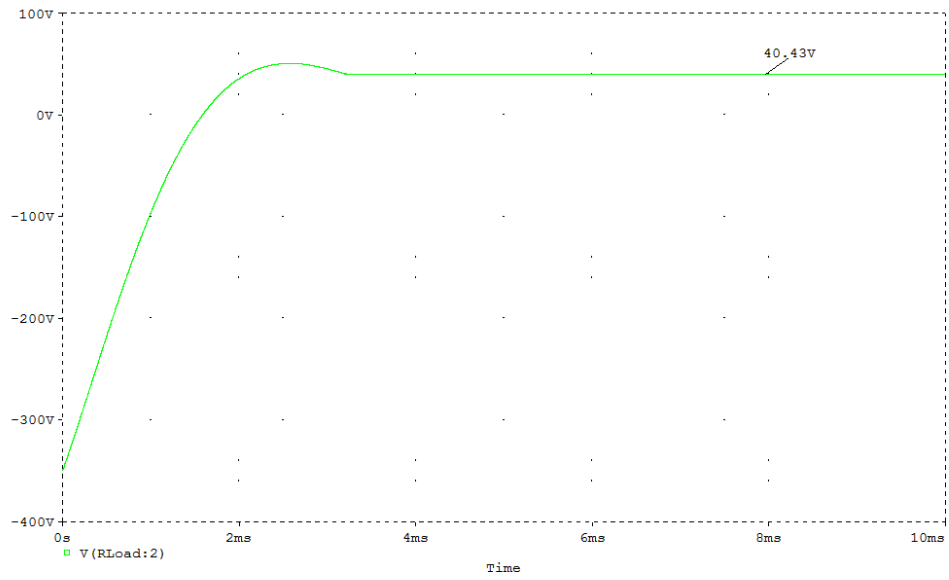


Figure 52: Converter output waveform for $F_s=180 \text{ kHz}$

For $F_s = 190 \text{ kHz}$;

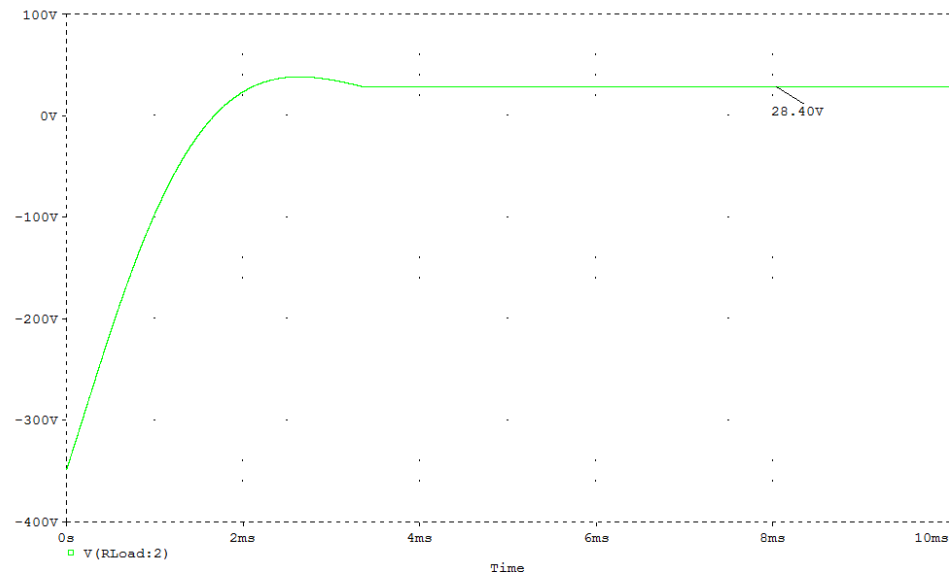


Figure 53: Converter output waveform for $F_s=190 \text{ kHz}$

For $F_s = 200$ kHz;

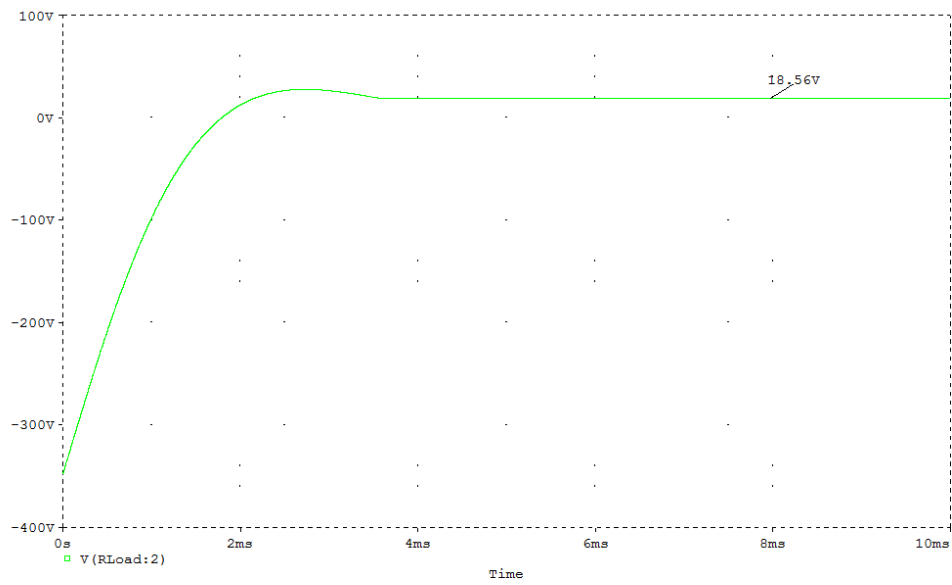


Figure 54: Converter output waveform for $F_s=200$ kHz

For $F_s = 210$ kHz;

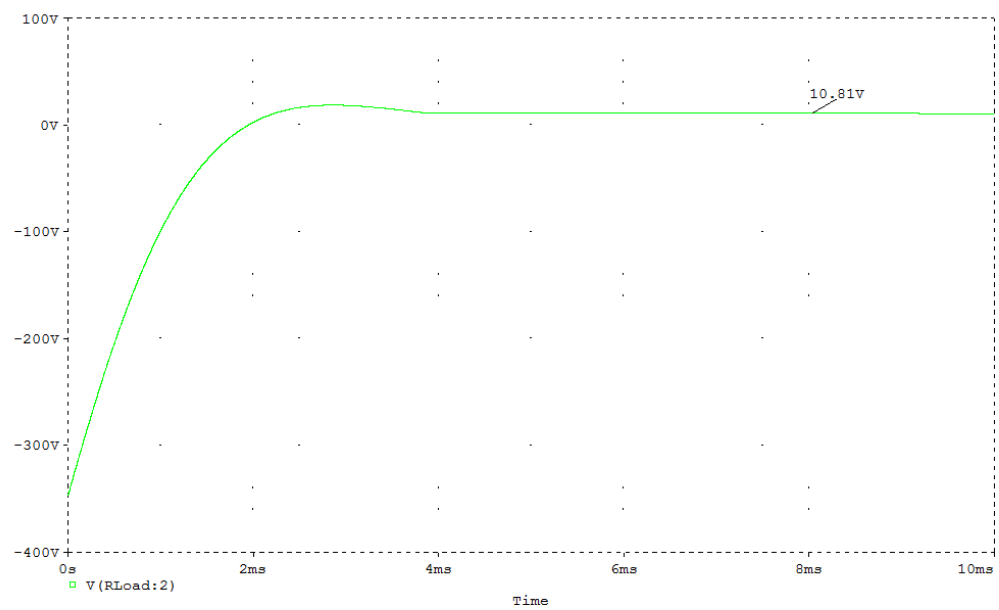


Figure 55: Converter output waveform for $F_s=210$ kHz

For $F_s = 220$ kHz;

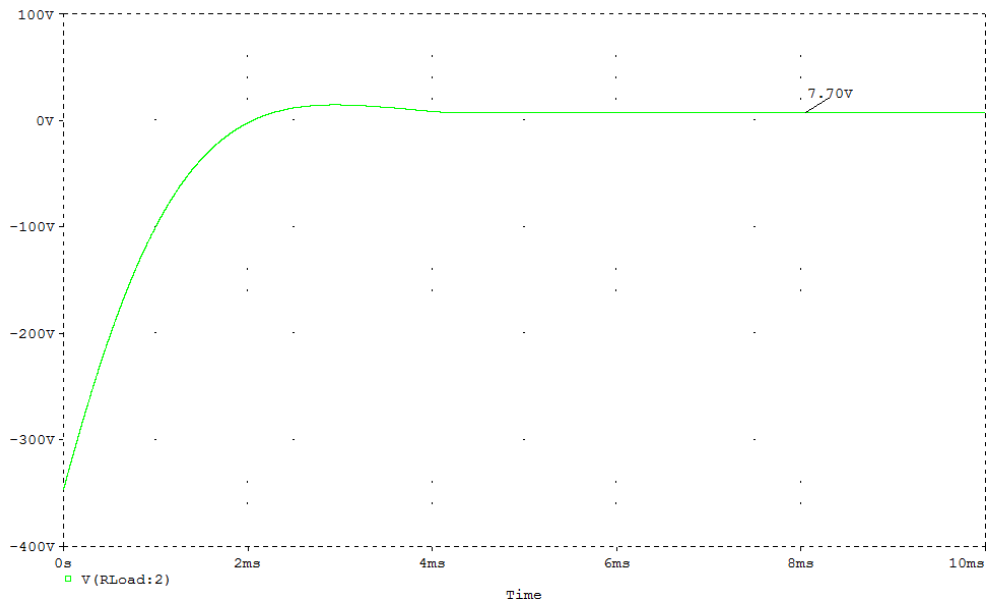


Figure 56: Converter output waveform for $F_s=220$ kHz

For $F_s = 230$ kHz;

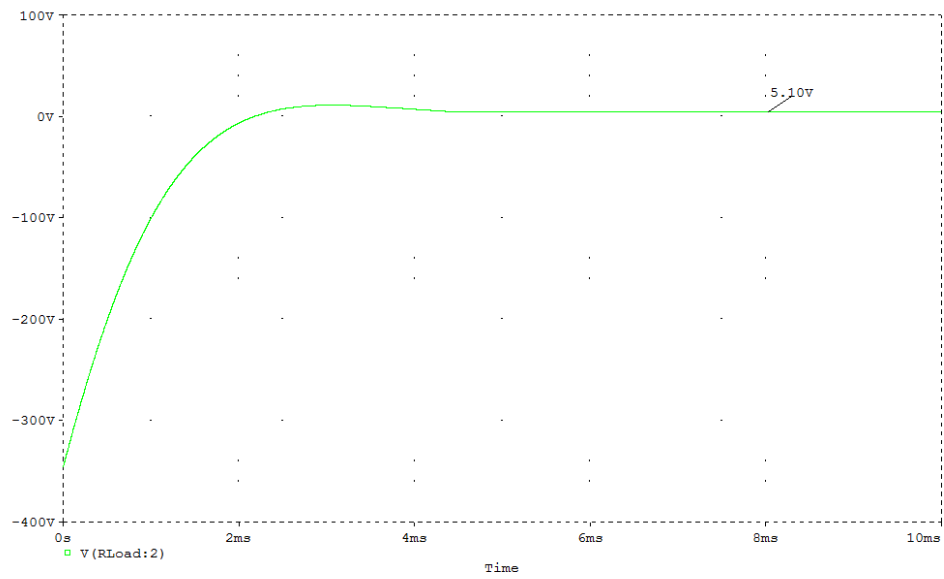


Figure 57: Converter output waveform for $F_s=230$ kHz

The converter output voltage value for every different switching frequency values is tabulated in the table below:

No.	Switching Frequency (kHz)	Output Voltage (V)
1	100	249.67
2	110	207.62
3	120	171.72
4	130	140.86
5	140	114.28
6	150	91.37
7	160	71.66
8	170	54.78
9	180	40.43
10	190	28.4
11	200	18.56
12	210	10.81
13	220	7.7
14	230	5.1

Table 7: Summary of variable DC output voltage

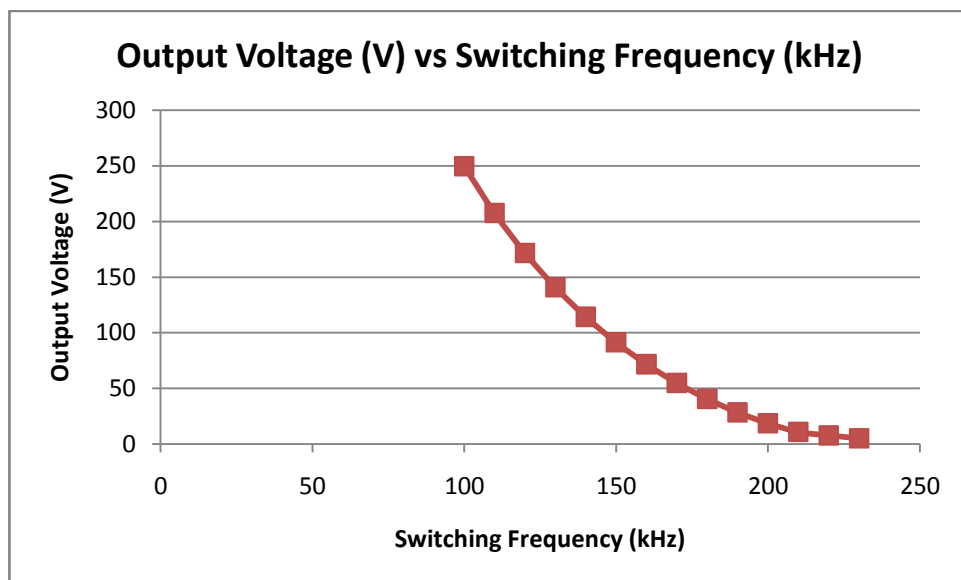


Figure 58: Converter output voltage characteristic for different F_s value

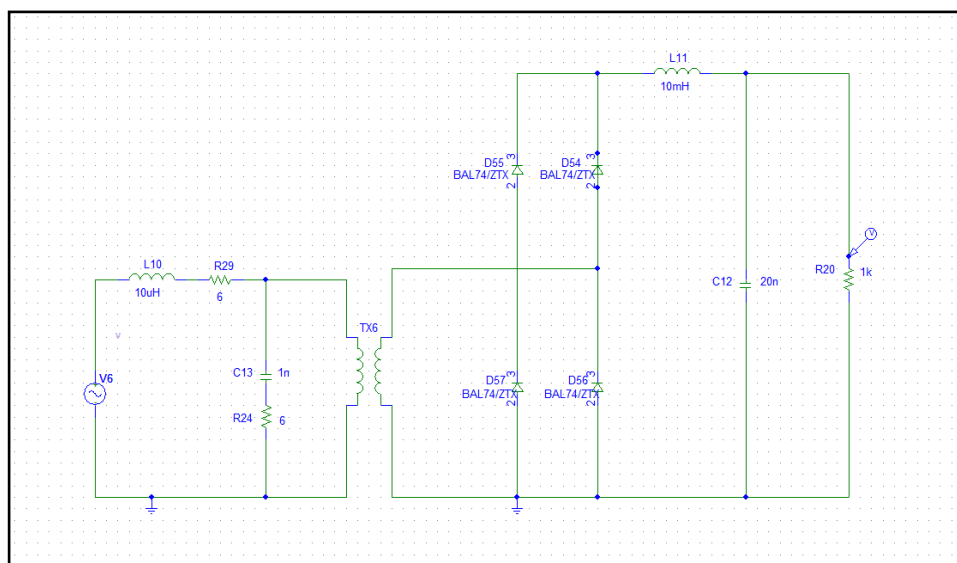
From the characteristics we observe that the output voltage varies as the value of switching frequency varies. The values of the output voltage then is compared with the voltage requirements for series of lithium ion battery.

Number of Lithium Ion Battery (Series)	Voltage Requirement
10	75.0 V
15	112.5 V
20	150.0 V
25	187.5 V
30	225.0 V

Table 8: Series of lithium ion battery voltage requirement

Notice that the range of output DC voltage of the converter circuit is ranging from 5.1V to 249.67V while for lithium ion battery specifications the range of voltage requires are ranging from 75V to 225V. Therefore the range of output voltage obtained is acceptable.

4.4 Results and Discussion for Rectifier at Very High Frequency



Above is the rectifier configuration. The frequency value is very high which is 13.5MHz. Output waveform for the rectifier is obtained as shown in Figure 59.

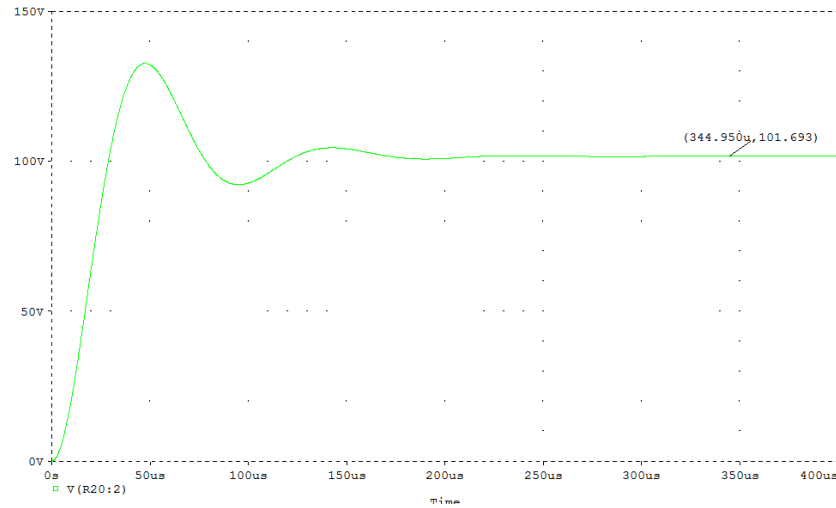


Figure 59: Waveform output voltage of the rectifier circuit

From the waveform, a smooth DC voltage is successfully obtained with no voltage ripple or noise. This waveform characteristic is acceptable but the value is not reaching desired value which is 340V. The highest voltage that could be obtained from the rectifier is 101.7V. This may be because of a very high frequency value at the input V6. In the modeled system, it is not suitable to use such very high frequency to simulate. Furthermore, for a very high frequency such as 13.5MHz, the switching will be very fast and this will affect the value of output voltage.

CHAPTER 5

CONCLUSION AND RECOMMENDATION

5.1 Conclusion

The project is smoothly progress according to the pre-planned methodology of FYP 1 and FYP2 Gantt charts which guide the project progress flow very well. According to the results and discussions made, the expected variation of output parameters with different switching frequency is observed and analyzed to choose the best switching frequency to be chosen. After getting the best switching frequency which gives the minimum value of switching losses, the project proceed by expanding the circuit with a transformer and connect it to a rectifier and a filter in order to obtain a DC voltage output. Analysis has been made and the output of the converter gives a variable DC voltage for different switching frequency.

Therefore, the objective to control the DC voltage output by changing the switching frequency value is achieved. From the modeled circuit design, it is proven that the converter design can be used for wireless power transfer in electric vehicle battery charging system.

We can conclude that the calculation of switching power losses is very significant in this project in order to design appropriate features of the converter circuit because the converter is dealing with high switching frequency.

As a conclusion, this project is a comprehensive research study about wireless power transfer in the electric vehicle battery charging system. The project is related to the study on electric vehicle battery charging system which is improving the practicality of plug-in charger cable usage in the electric vehicle industries.

5.2 Recommendation

It is recommended in this project to provide a controller device that can be applied to control the switching frequency so that the converter circuit will produce a specific output voltage according to the capacity of electric vehicle battery. This is because the voltage required for the battery at a time will be different depending on the value of voltage discharged during electric vehicle operation. Besides that, it is also recommended for the project to install an auto power cut-off system such as circuit breaker close to the battery to minimize the risk of failure of the system during accident.

Other than that, for a very high frequency source, such as 13.5MHz, the rectification could be improved using other rectification design approach. This is because of the very fast of switching which effects on low voltage. It may also work if the circuit is provided with a voltage booster at the output to boost up the voltage in order to get the desired voltage output. From all the findings and analysis, further research studies could be conducted to improve the converter design.

REFERENCES

- [1] EUCAR: The electrification of the vehicle and the urban transport system, European Automotive Manufacturers, 2009.
- [2] Chwei-Sen Wang, Stielau O.H., Covic G.A.: Design considerations for a contactless electric vehicle battery charger, *IEEE Transactions on Industrial Electronics*, 52(5), pp.1308 - 1314, 2005.
- [3] Pedder D.A.G., Brown A.D., Skinner J.A.: A contactless electrical energy transmission system, *IEEE Transactions on Industrial Electronics*, 46(1), pp. 23 - 30, 1999.
- [4] Chang-Gyun Kim, Dong-Hyun Seo, Jung-Sik You, Jong-Hu Park, Bo-Hyung Cho: Design of a contactless battery charger for cellular phone, *Fifteenth Annual IEEE Applied Power Electronics Conference and Exposition - APEC 2000*, Vol. 2, pp. 769 - 773, 2000.
- [5] Zhang Bingyi, Liu Hongbin, Zhao Yisong, Ying Yong, Feng Guihong: Contactless electrical energy transmission system using separable transformer, *Proceedings of the Eighth International Conference on in Electrical Machines and Systems - ICEMS 2005*, Vol. 3, pp. 1721 - 1724, 2005.
- [6] Ayano H., Yamamoto K., Hino N., Yamato I.: Highly efficient contactless electrical energy transmission system, *IEEE 28th Annual Conference of the Industrial Electronics Society - IECON 02*, Vol. 2, pp. 1364 - 1369, 2002.
- [7] Qingxin Yang, Jianguai Li, Haiyan Chen, Junhua Wang: Design and analysis of new detachable coreless transformer used for contact-less electrical energy transmission system, *IEEE Vehicle Power and Propulsion Conference - VPPC '08*, pp. 1 - 4, 2008.
- [8] Jun Liu, Licheng Sheng, Jianjiang Shi, Zhongchao Zhang, Xiangning He: Design of high voltage, high power and high frequency transformer in lcc resonant converter, *Twenty-Fourth Annual IEEE Applied Power Electronics Conference and Exposition - APEC 2009*, pp. 1034 - 1038, 2009.

- [9] Sallan J., Villa J.L., Llombart A., Sanz J.F.: Optimal design of icpt systems applied to electric vehicle battery charge, *IEEE Transactions on Industrial Electronics*, 56(6), pp.2140 - 2149, 2009.
- [10] Chunbo Zhu, Kai Liu, Chunlai Yu, Rui Ma, Hexiao Cheng: Simulation and experimental analysis on wireless energy transfer based on magnetic resonances. *IEEE Vehicle Power and Propulsion Conference -VPPC '08*, pp. 1-4, 2008.
- [11] Byung-Song Lee, Kyung-Hee Han: Modeling and analysis of IPT system used for PRT, *Proceedings of the Eighth International Conference on Electrical Machines and Systems - ICEMS 2005*, Vol. 1, pp. 839 - 842, 2005.
- [12] Chwei-Sen Wang, Covic G.A., Stielau O.H.: Power transfer capability and bifurcation phenomena of loosely coupled inductive power transfer systems, *IEEE Transactions on Industrial Electronics*, 51(1), pp.148 - 157, 2004.
- [13] Wang C.-S., Stielau O., Covic G.: Design considerations for a contactless electric vehicle battery charger, *IEEE Transactions on Industrial Electronics*, Vol. 52, no. 5, pp. 1308 - 1314, 2005.
- [14] <http://www.designworldonline.com/a-new-way-to-charge-electric-vehicles/>
- [15] A. K. Panda, Aroul. K, "A Novel Technique to Reduce the Switching Losses in a Synchronous Buck Converter", *International Conference on Power electronics,drives and Energy System, PEDES*, December 2006.

APPENDIX

APPENDIX A

Battery Specifications:

1. Unit Cell Design

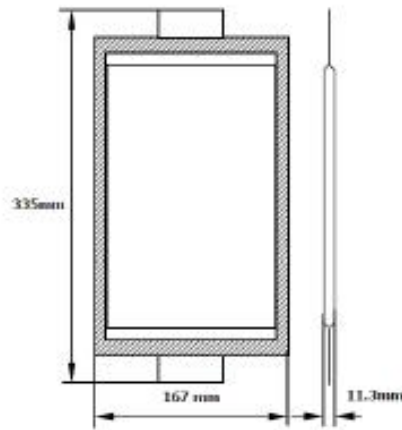


Figure 1: Cell dimension (43AH, 3.75V)

2. Unit Module Design



Figure 2: Unit Module – contain 4 cells (2S2P)

3. Unit Module Specification:

Table 1: Summary of the unit module specification

Item	Specification
Weight	≤4.8kg
Normal capacity	86 Ah @ 0.5C
Capacity Range	SOC10 ~ SOC95 (85% Usable)
Normal voltage	(1C) 7.5 V
Charging cut-off voltage	8.30 ± 0.05 V
Discharging cut-off voltage	6.00 ± 0.05 V
Standard charging current	1C
Standard discharging current	1C
Max continuous charging current	172A
Max continuous discharging current	460A @ SOC50, 30sec, 25°C
Max plus discharging current	600 A
Energy density	160 Wh/kg
Power density (SOC50, 10sec, 25°C)	1.813 W/kg
Internal resistance	1.64 mΩ (SOC50, 30sec Discharge)
Charge working temperature	-20 ~ 50°C
Discharge working temperature	-20 ~ 50°C
Storage temperature	-40 ~ 60°C
Appearance	Thickness : 53.6 mm Width : 184.2 mm Length : 360.2 mm As shown in Figure 2

4. Battery Specification (University will supply 13 units of Unit Module)

- a. Configuration of unit module : 13 series
- b. Capacity (0.5C) : 86AH
- c. Operational Voltage (0.5C)
 - i. Charging mode – upper limit : 107.9V
 - ii. Discharging mode – lower limit : 78.0V
 - iii. Discharging mode – nominal : 97.5V

d. Picture of battery in 13S array:

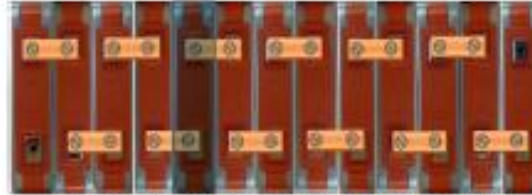


Figure 3: Top view battery in 13S array



Figure 4: Side view of battery in 13S array

5. Safety consideration

- a. The Battery Management System (BMS) is compulsory when unit module connect in series mode.
- b. Battery is needed to operate within the specification voltage range, and overcharging will cause explosion or fire. For this purpose, BMS is required especially during charging mode.
- c. Proper size of bus-bar connectors, cable and vibration type screw are required to minimal energy loss and safety.
- d. Battery is needed to pack in fire casing and cooling using air flow.
- e. To minimize risk of failure during accident, the auto power cut-off system (eg. Circuit breaker, etc) must be installing close to battery (energy source).